Title: Hygrothermal calibration and validation of vernacular dwellings: a genetic algorithm-based optimisation methodology

Inês Costa-Carrapiço [a, *], Ben Croxford [b], Rokia Raslan [b], Javier Neila González [a]

[a] *Departamento de Construcción y Tecnología Arquitectónicas, Escuela Técnica Superior de Arquitectura, Universidad Politécnica de Madrid, Avenida Juan de Herrera 4, 28040 Madrid, Spain*

[b] *UCL Institute of Environmental Design and Engineering, University College London, 14 Upper Woburn Pl, London WC1H 0NN, UK*

* Corresponding author at *Universidad Politécnica de Madrid, Avenida Juan de Herrera 4, 28040 Madrid, Spain.* E-mail address: ines.costa.carrapico@gmail.com (I. Costa Carrapiço) ORCID 0000-0003-4921-0538

Abstract

Heritage model calibration and validation are crucial for decreasing uncertainty and enhancing the robustness of simulation results and conservation interventions. Yet, hygrothermal modelling methodologies are marked by significant heterogeneity and lack of robustness. Aiming to provide a solution for the drawbacks identified, this study puts forth a comprehensive hygrothermal modelling methodology. Following the *in situ* data collection of a subset of heritage buildings, 22 vernacular dwellings in Southern Portugal, a three-step method was developed, consisting of: Morris sensitivity analysis, optimisation-based calibration, and validation and multi-criteria decision-making (MCDM). A genetic algorithm multi-objective optimisation-based calibration with NSGA-II was implemented for simultaneously minimising the statistical indicators RMSE and MAE for the indoor air temperature of the winter and summer models. The validation and MCDM were conducted by means of threshold compliance and Compromise Programming. NSGA-II found Pareto frontiers composed of nine and six optimal solutions for the summer and winter models, respectively, in nearly three hours each. All optimal solutions significantly decreased the RMSE and MAE, especially in the summer model, regarding the baseline data. The final solutions selected after the MCDM resulted in an accuracy improvement of 51 % and 54 % for the RMSE and MAE for the winter model and 80 % and 81 % for the RMSE and MAE in the summer model, compared to the baseline models. The strong correlation found between the calibrated models and the measured data along with the enhancement of calibrated data regarding the baseline model, highlighted the potential of using GAs to obtain calibrated vernacular models that robustly predict real building performance and foster better retrofitting decision-making.

Keywords: Simulation model calibration; Hygrothermal model validation; Vernacular dwellings; Genetic algorithm; Multi-objective optimization.

1

1. Introduction

Vernacular dwellings are inherently linked to their environmental context and available resources, and built to meet specific needs using traditional technologies while accommodating the values, economies, and ways of life of the cultures that produce them [1,2]. Currently, the dynamic thermal simulation of these types of dwellings is an expanding research field with extensive potential for, *inter alia*, obtaining long-term performance predictions, performing sensitivity and parametric analyses, and examining climate change resilience and its impact on thermal comfort [3,4]. Since the research interest on this topic peaked in 2014, 26 studies have been published on modelling vernacular dwellings [5–34], of which 19 focus on thermal comfort evaluation [6,11,14–17,21,22,35–45] by combining simulation and *in situ* monitoring, with EnergyPlus via the DesignBuilder interface being by far the most employed [4]. Moreover, a systematic review of vernacular dwellings' climate responsiveness was recently published, confirming the research trend of coupling fieldwork with simulation for evaluating climate responsiveness and the effectiveness of strategies, with EnergyPlus via DesignBuilder being the main simulation software, followed by Ecotect, Phoenics and eQuest [46]. In addition, two publications contributed to the analysis of research challenges and recommendations in dynamic thermal and hygrothermal simulation and validation of historical buildings [3,47].

The thermal simulation of vernacular dwellings presents specific challenges linked with **a lack of consistent validation methodology or guidelines for hygrothermal model calibration**, **input-data dependent model accuracy, the gap between modelled and actual conditions, and software limitations for modelling complex vernacular architecture elements** [4]. An inaccurate modelling stage may lead to inappropriate conclusions and interventions, which in turn misinform the indoor thermal comfort assessment and the retrofitting decision-making process [47]. In this regard, thorough model calibration and validation are crucial for decreasing uncertainty and enhancing the robustness of the simulation results, as would be the scientific consensus on standard key parameters.

Currently, ASHRAE Guideline 14-2014 [48] stands out as the most followed validation method, suggesting two main statistical indicators for model validation according to hourly or monthly data: the Coefficient of Variation of the Root-Mean-Square Error ((CV)RMSE) and the Mean Bias Error (MBE) or the Normalised Mean Bias error (NMBE).

Abbreviations: CoP: Coefficient of performance; CP: Compromise Programming; (CV)RMSE: Coefficient of Variation of the Root-Mean-Square Error; GA: Genetic Algorithm; IAQ: Indoor Air Quality; LV1/2: Level 1/2; MAE: Mean Absolute Error; MBE: Mean Bias Error; MCDM: Multi-criteria decision-making; MOEAs: multi-objective evolutionary algorithms; MOO: Multi-objective optimisation; NMBE: Normalised Mean Bias Error; NSGA-II: Non-dominated Sorting Genetic Algorithm; RH: Relative Humidity; RMSE: Root Mean Square Error; SA: Sensitivity Analysis; SVV: São Vicente e Ventosa; T_a: Air temperature; T_g: Globe Temperature; T_{mrt}: Mean Radiant Temperature; T_s: Surface; V_a: Air velocity.

Alternatively, the FEMP [49] and IPMVP [50] criteria may be adopted for validating building simulation models. All three guidelines take an energy-based approach to the validation process. Thus, **thermal comfort studies in vernacular dwellings default to adapting the criteria for predicted energy consumption, using the monitored environmental parameters in place of the energy data** [4,47], leading to a **high degree of dispersion amongst vernacular modelling studies, with no clear framework, and heterogeneity of indexes, control parameters, validation periods and thresholds.** This hampers the comparative analysis and replicability of findings in this field [51], increases uncertainty, and impacts trust in research, stressing the need for heritage-adequate indexes. Moreover, the most used statistical indicators for model validation in vernacular dwellings present some **drawbacks related to the error cancellation effect and results dependent on the dataset scale due to the normalisation process, leading to possible misinterpretation** [47,52,53]. Additionally, these **indicators have recently been suggested as unsuitable for heritage buildings** [47], finding that the combination of the Mean Absolute Error (MAE) and the Root Mean Square Error (RMSE) would be more reliable, i.e. allowing to avoid misinterpretation due to the normalisation process and with RMSE, in particular, having a high sensitivity to the amplitude of residuals which can be more suitable to heritage buildings [47]. Moreover, based on the review conducted in [4], **a robust and time-efficient hygrothermal calibration technical process is yet to be explored in vernacular dwellings modelling research**, and by the same token, to the best of the authors' knowledge, **simultaneously targeting the minimisation of the gap between modelled and monitored data through two heritage-adequate error indexes is yet to be conducted in this type of buildings**.

Thus, further research is essential through studies focusing on modelling vernacular dwellings and their accurate and efficient calibration and validation, to **help bridge the modelled-real performance gap. Research developing a common framework based on heritage-adequate error indexes would be essential for furthering the robustness of this research niche, by obtaining accurately validated models, which would allow to determine adequate interventions with real-world implications at the heritage conservation level.**

1.1. Aim and objectives

The present study is part of a larger study [54,55] assessing rural vernacular dwellings established in São Vicente e Ventosa (SVV), Alentejo, Portugal. Its overarching purpose is to put forth a modelling and hygrothermal calibration and validation framework for vernacular dwellings, which could contribute towards overcoming the main issues identified in previous studies.

In achieving this goal, the following specific objectives were set:

i. Building the case studies baseline models fed with *in situ* data from the as-built survey, environmental and thermophysical monitoring, and occupant surveying;

ii. Conducting a Sensitivity Analysis (SA) to ascertain the models' parametric effect on the statistical error indicators MAE and RMSE regarding indoor air temperature and, thus, reducing the number of parameters for the optimisation-based calibration;

iii. Carrying out a multi-objective optimisation-based calibration of the models simultaneously targeting the minimisation of the heritage-adequate indexes MAE and RMSE, using GA;

iv. Validating the models based on accuracy threshold compliance regarding the error indicators MAE and RMSE and the Residuals Frequency Analysis, based on indoor air temperature, surface temperature, and Relative Humidity;

v. Conducting Pareto multi-criteria decision-making via Compromise Programming to obtain the final calibrated and validated models.

2. Materials and methods

The case studies as-built survey, *in situ* environmental and thermophysical monitoring, and occupant surveying conducted prior to the modelling stage were described in depth in [54,55]. Figure 1 illustrates the methodology developed for modelling the case studies.

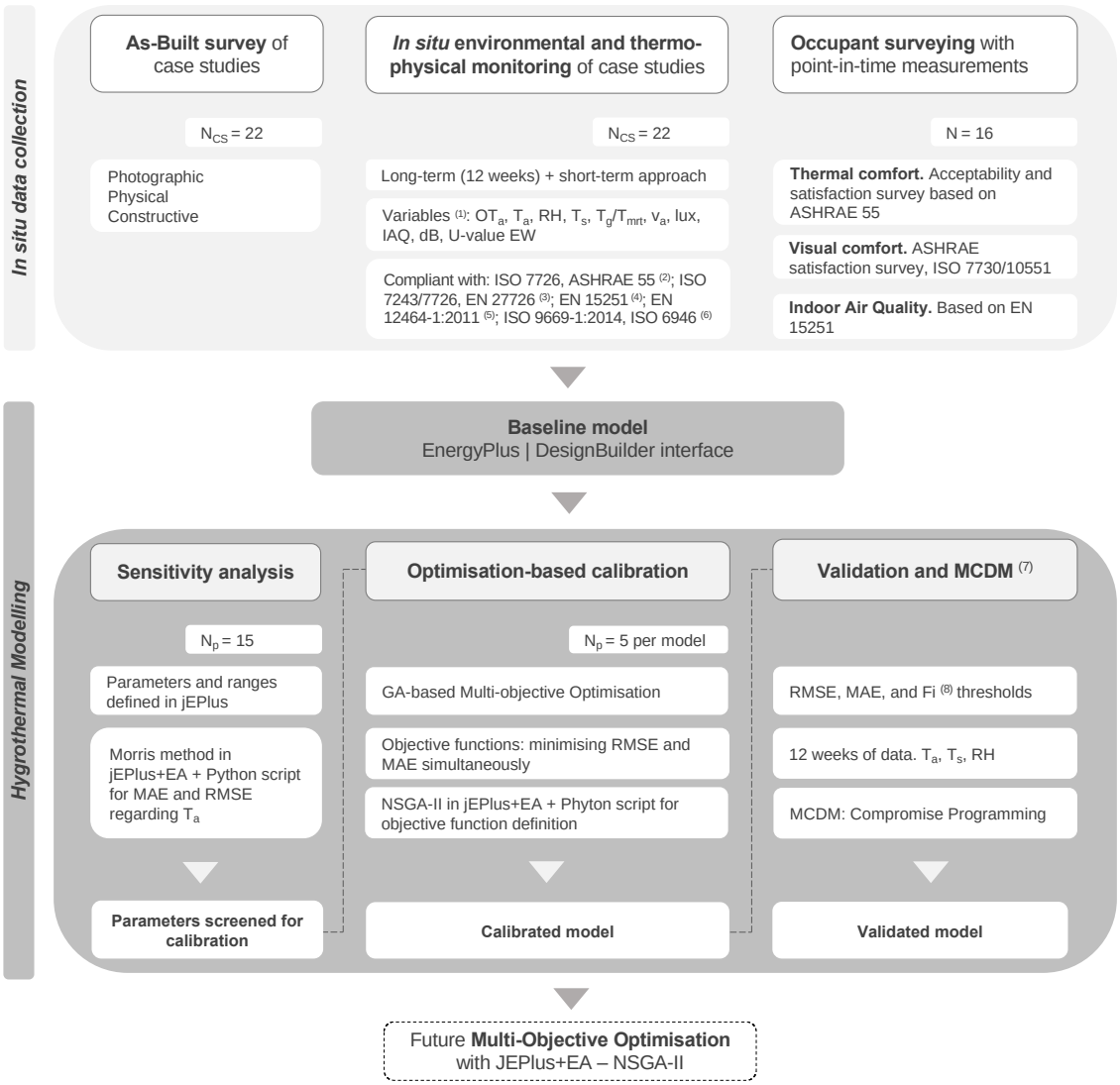

(1) OT_a: Outdoor Air Temperature; T_a: Indoor Air Temperature; RH: Relative Humidity; T_s: Surface Temperature; T_g: Globe Temperature; T_{mrt}: Mean Radiant Temperature; V_a: Air Velocity; Lux: Natural illuminance; IAQ: Indoor Air Quality; dB: Sound level; U-value EW: Thermal Transmittance of the external walls; (2) T_a, RH, and V_a; (3) T_{mrt}; (4) IAQ, Lux, dB; (5) Lux; (6) U-value; (7) MCDM: Multi-criteria Decision-Making; (8) Fi: Residuals Frequency Analysis.

Fig.1. Methodology developed for the hygrothermal modelling of the vernacular case studies.

2.1. Brief description of the case studies

The vernacular case studies are established in SVV, which is characterised by a temperate climate, with dry and hot summer, sub-type Csa of the Köppen Climate Classification [56]. The typical case study layout (70 % of the case studies) is a rectangular floor plan with average dimensions of 6.00 m x 10.00 m, divided into two main spaces: a sleeping space and a living space, where all indoor activities take place. The heavy thermal mass walls built in limestone and earth masonry with lime wash finish have an average thickness of 0.60 m. The roof is composed of single hollow clay bricks and Arabic tiles, and the ground is made of ceramic floor tiles. The significantly-sized fireplace and chimney play a predominant role in the case studies and their lack of windows in all walls are amongst their key bioclimatic features. Further details can be found in [54].

2.2. *In situ* monitoring and surveying

22 vernacular dwellings were selected for the as-built survey, summer and winter *in situ* monitoring (three months), and occupant surveying. The criteria for selection were the following: i. representativeness of regional vernacular dwellings and their bioclimatic strategies; ii. preservation of traditional building elements, including the façade's integrity; iii. residential occupancy; iv. physical condition. To this end, a photographic survey of the façades of the entire settlement was carried out, resulting in 75 preliminary options, which decreased to 22 final ones due to additional considerations, i.e. access denied by occupants, abandonment or construction work; absence of occupants; modified indoor space and construction systems. The parameters measured included outdoor and indoor air temperature (T_a), relative humidity (RH), globe temperature (T_g), surface temperature (T_s), air velocity (V_a), illuminance, indoor air quality (IAQ), and sound level. The survey focused on thermal perception and acceptability, and IAQ and illuminance. The respective methodologies and findings were discussed in [54,57] and the details of the measurements conducted are listed in the Appendix A.

The summer *in situ* experimental measurements of the U-values were measured on south-west-facing external walls, simultaneously with the T_s, T_a, and outdoor air temperature monitoring, in three case studies, for 72 hours, duly shielded against thermal radiation, ventilated, and mounted so as to ensure a result representative of the whole element, as established in ISO 9869-1:2014 [58]. No previous thermographic investigation was conducted as acknowledged in the limitations section of the paper. The measurement was conducted with a calibrated Multifunction Testo 435-2 probe with a triple sensor system for the wall temperature, which computes the U-value according to the ISO 6946:2017 [59]. The

three-day monitoring time was established according to ISO 9869-1:2014, as the walls met the condition of thermal stability before and during the measurement, which was verified with the probe [58,60].

2.3. Baseline model settings

The baseline model was built for the most common strategies used in the case studies for coping with heat in the cooling season and cold in the heating season, i.e. natural ventilation supplemented by mechanical ventilation, and electric heating, respectively, as evidenced in the monitoring stage [54], and based on the typical case study described in section 2.1.. Starting from the as-built survey technical drawings in Autodesk AutoCAD, the models were developed with EnergyPlus v8.9.0. via DesignBuilder v6.1.6., due to being the most employed software for modelling vernacular dwellings [4]. Table 1 summarises the input data of the models informed by the *in situ* monitoring and physical survey. Regarding weather data, and despite its considerable impact on the simulation outputs' accuracy, the overwhelming majority of vernacular modelling studies use the nearest reference weather station template with historical meteorological national data, contributing to increased uncertainty and model inaccuracies [4,36]. In this study, the authors used Elements v1.0.6., an open-source cross-platform software tool to edit custom weather files for building modelling, to edit the EnergyPlus Weather File of the case studies' nearest station (Badajoz) according to the outdoor data collected *in situ*. Figure 2 displays the comparison between the edited weather file informed by the *in situ* weather data measurements and the Badajoz weather station template.

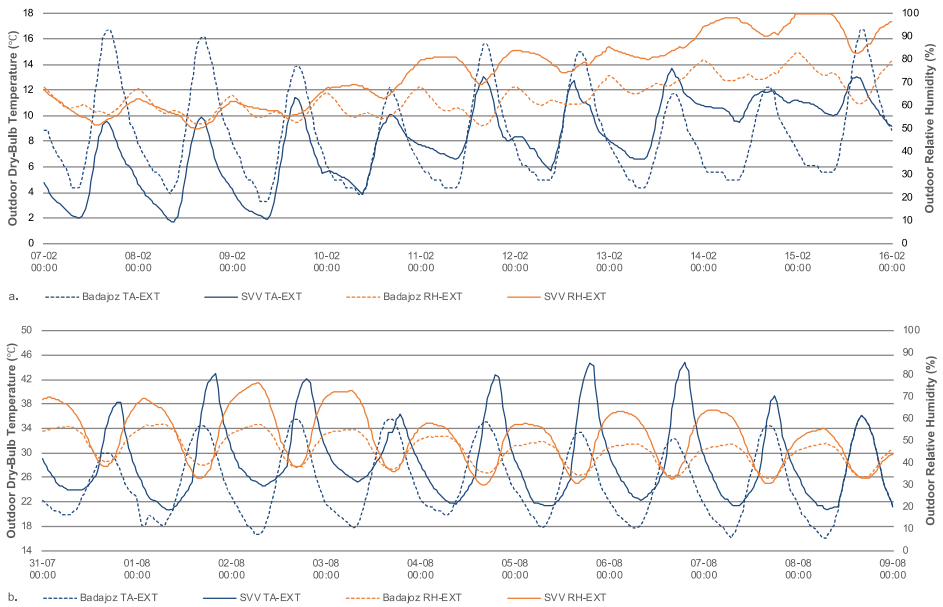

Fig. 2. Comparison between Badajoz's template weather file and the edited weather file informed by the *in situ* climate data measurements in SVV, in winter (top) and summer (bottom).

2.4. Model calibration and validation

A three-step approach illustrated in Fig. 1, and whose technical mechanisms are detailed in Fig. 3, was implemented for validating the case study models, composed of: sensitivity analysis, calibration and validation, and multi-criteria decision-making (MCDM).

2.4.1. Sensitivity analysis (SA)

The Morris SA [61] was conducted to reduce the calibration parameters. Exploring the full input space (1.073.741.824 possible iterations) with EnergyPlus's parametric shell, i.e. jEPlus, proved to be computationally-prohibitive. Thus, the Morris or elementary effects method, based on the One-at-a-Time (OAT) design [62] for global SA, was chosen for being the most used in building performance [63–68], providing greater reliability and a more comprehensive impact of input uncertainty on output performance than local SA methods [69–72], and a good accuracy-efficiency trade-off [68]. The main aim was to ascertain the models' parametric effect on the statistical error indicators MAE and RMSE regarding indoor air temperature (T_a). T_a was selected over RH due to the latter's dependency on the former. As mentioned in the introductory section, the most used indexes for vernacular model validation have been deemed unsuitable for hygrothermal model validation of heritage buildings.

Table 1. Summary of the baseline models settings.

Settings	Parameters	Input data	Source of baseline data
General settings	Weather data	Modified EPW template	*In situ* long-term monitoring [54]
	Geometry	Drawn in AutoCAD	As-built survey [39]
	Air velocity	0.15 m/s	*In situ* long-term monitoring
	Calculation options	4 time steps for naturally-conditioned models	Software recommendation
		6 time steps for mechanically-conditioned ones	Software recommendation
Construction settings			
External and internal walls	Thickness (m)	0.60	As-built survey; *in situ* experimental measurement; Portuguese tradicional
L1 Lime sand render; L2 Soft	U-value ($W/m^2.K$)	1.273 (EW) / 1.172 (IW)	construction systems handbook [73]; ISO 10456 [74]; ISO 9869-1:2014 [58]
limestone and earth gravel masonry;	R-value ($m^2.K/W$)	0.786	
L3 Lime plaster			
Roof	Thickness (m)	0.12	Portuguese traditional construction systems handbook; ISO 10456
L1 Single hollow clay Arabic tile;	U-value ($W/m^2.K$)	3.13	
L2 Lime mortar; L3 Arabic tile	R-value ($m^2.K/W$)	0.345	
Ground	Thickness (m)	0.04	Portuguese traditional construction systems handbook; ISO 10456
L1 Ceramic tiles; L2 Lime mortar;	U-value ($W/m^2.K$)	1.53	
L3 Earth	R-value ($m^2.K/W$)	0.17	
Envelope	Airtightness	0.8 ac/h average constant rate; 24/7 schedule	Technical literature [5]
	Linear thermal bridging, Psi values:		Software default value based on BRE IP 1/06 [75]

	Roof-wall (W/m.K)	0.18	
	Wall-ground floor (W/m.K)	0.24	
	Wall-wall (W/m.K)	0.14	
Cooling | Heating settings			
Convection algorithms	Inside convection	TARP convection algorithm	Default based on ASHRAE algorithms
	Outside convection	DOE-2 convection model	Default based on MoWitt and BLAST detailed convection models [76]
Heating data			
Fireplace and wood stoves	Heating fuel	Dual fuel appliances (mineral + wood)	Monitoring data [54]
	Air temperature distribution	Mixed	Monitoring data; ISO 7726 [77]
	Heating schedule	07:30 – 23:00	Occupant survey [55]
Electric	Heating fuel	Convective, electricity from grid	Monitoring data [54]
	Air temperature distribution	Mixed	Monitoring data; ISO 7726 [77]
	Heating schedule	07:30 – 23:00	Occupant survey
	Energy consumption (kWh/m^2/month)	3	Occupant survey
	CoP (Coefficient of Performance)	0.89	Software default value
Unheated	-	-	
Cooling data			
Natural ventilation	Definition method: min fresh air per person (l/s)	2.5	ASHRAE 62.1-2013, Addendum 2015 [78]
	Schedule	07:00-09:00/22:00-23:00	Occupant survey
	Delta T and wind speed coefficients	Constant at 0.4	Software default value
	Air distribution mode	Mixed	Monitoring data; ISO 7726 [77]
Mechanical ventilation	Schedule in living room	12:00-22:00	Occupant survey
	Definition method: min fresh air per person (l/s)	2.5	ASHRAE 62.1-2013, Addendum 2015 [78]
Other gains	Miscellaneous: power density (W)	350	Software default value

	Radiant fraction	0.2	Software default value
Comfort radiant temperature weighting	Mean radiant temperature calculation	Zone averaged	Software recommended method for spaces with no windows
Lighting settings	Normalised power density (W/m^2/100 lux)	5.0	Occupant survey
	Luminaire type	Suspended	Occupant survey
	Radiant fraction	0.42	Software default value
	Visible fraction	0.18	Software default value
	Schedule	ON 12:00-13:00; 21:00-23:00	Occupant survey
	Lighting target (lux)	20	Monitoring data; EN 17037 [79]
Occupancy settings			
Activity and metabolic rate	Living room miscellaneous (met) (W/m^2)	2.0 | 115	ASHRAE 55-2013 [80]; occupant survey
	Seated, quiet/watching TV (met) (W/m^2)	1.0 | 60	
	Bedroom sleeping (met) (W/m^2)	0.7 | 40	
Clothing	Winter living room/bedroom (clo)	1.3 | 1.5	ASHRAE 55-2013; occupant survey
	Summer living room/bedroom (clo)	0.54-0.57	
Occupancy schedule	Living room	07:30/23:00, 7 days per week	Occupant survey
	Bedroom	23:00/07:00, 7 days per week	
Occupancy density	Living room/bedroom (people/m^2)	0.096/m^2 (2 people for 20,91 m^2)	Occupant survey

Hence, this research adopted the error statistical indicators recommended for heritage buildings in [47], for assessing the difference between the dwellings' *in situ* monitored and simulated T_a. The dwellings' main living area was chosen as the single thermal zone for calculations.

For each parameter, the Morris method computes the average of the absolute value of elementary effect (EE) on the objectives, which is an indicator of the parameters' influence on the output. The EEs, i.e. approximations of the first-order partial derivatives of the model [68], are estimated at sampled points randomly selected from a grid of values resulting from the parameter space discretisation based on the parameter division into a chosen number of levels. Starting from a grid basepoint, a step is taken, with random trajectory, by varying one parameter value at a time. With each step an EE value is obtained matching the change in the model outcome from varying one input value. The distributions of the first-order EEs for the whole parameter set can then be used for ranking purposes, as the two sensitivity indexes obtained, i.e. mean (μ) and standard deviation (σ) of the EEs, allow for input parameters to be classified into three groups: negligible effects, large linear effects without interactions, large nonlinear or interaction effects [81]. A further index, μ*, displaying the total effects of the input factor, has been introduced [72,82].

Table 2 showcases the 15 screening parameters, along with the baseline values and respective ranges defined according to presumed uncertainty and the technical literature. This process was established in jEPlus v2.1.0. and then run in jEPlus+EA v2.1.0. and EnSimS for the Morris SA. A script in Python v3.10 was integrated for optimising the MAE and RMSE calculation, which were computed per the following formulas given in [47]:

(1) $MAE = \frac{\sum_{i=1}^{n}|m_i - s_i|}{n}$

(2) $RMSE = \sqrt{\frac{\sum_{i=1}^{n}(m_i - s_i)^2}{n}}$

Where n is the number of data samples, m_i refers to the measured data, and s_i is the simulated data.

Table 2. Summary of the baseline models settings.

N	Element	Variables	Baseline data	Range for SA
P4	**External wall**	U-value (W/m^2.K)	1.273	1.0 – 1.6
P1		Density (kg/m^3)	1800	1300 - 2500
P2		Specific heat (J/kg.K)	900	600 - 1000
P3		Thermal absorptance (0-1)	0.9	0.7 – 0.95
P5	**Partition wall**	U-value (W/m^2.K)	1.273	0.9 – 1.4
P6		Density (kg/m^3)	1800	1300 - 2500
P7		Specific heat (J/kg.K)	900	600 - 1000
P14	**Roof**	U-value (W/m^2.K)	3.13	0.5 – 3.5
P13		Thermal absorptance (0-1)	0.9	0.7 – 0.95
P8	**Envelope**	Airtightness (ACH)	0.8	0.5 – 1.85

P11		Linear thermal bridging, Psi values [(1)]		
		Roof-wall (W/m.K)	0.18	0.04 – 0.5
		Wall-ground floor (W/m.K)	0.24	0.04 – 0.5
		Wall-wall (W/m.K)	0.14	0.04 – 0.5
P15	**HVAC**	Ventilation flow rate (l/s per person)	2.5	2.0 – 5.0
P12		Miscellaneous loads (W/m^2)	17	10.0 – 50.0
P9	**Occupancy density**	Number of people per area	$0.096/m^2$	0.05 – 0.15
P10	**Lighting**	Normalised power density (W/m^2 / 100 lux)	5.0	3.0 – 8.0

[(1)] See Table 1 for data source.

2.4.2. Calibration

Based on the findings of the SA regarding the most relevant parameters, a multi-objective optimisation-based calibration was implemented in jEPlus+EA v2 using a genetic algorithm (GA): the Non-dominated Sorting Genetic Algorithm (NSGA-II). A multi-objective optimisation (MOO) was chosen to simultaneously target both the statistical error indicators MAE and RMSE regarding T_a as the objective functions that guide the algorithm in the solution search. This was implemented by virtue of a second Python script automating the uncertainty analysis for each simulation according to the formulas presented in 2.4.1.. The reference periods for the calibration matched the *in situ* monitoring in 2015 [54], i.e. from July 5th to August 16th and from January 16th until February 27th, 2015. The models were calibrated separately due to the divergence in occupancy behaviour between summer and winter conditions, e.g. ventilation flow.

Genetic Algorithm simulation. GA is an evolutionary Pareto-based elitist strategy that successfully solves MOO problems by simultaneously optimising two or more objectives of conflicting nature [83]. Despite being common practice for decision-making in the building sector due to their relative simplicity, non-evolutionary-based methods exhibit drawbacks such as being limited to expert knowledge and best construction practice [84–87], partial solution assessment in trial-and-error simulation evaluations with no guarantee of finding optimal solutions [88–91], and the time-consuming feature of exhaustively searching the entire solution space [92–94], which inhibit their application in MOO problems [95]. The literature on GAs' performance suggests these are the most popular and robust heuristic approach to MOO problems in the field of building optimisation [84,88,96–117]. NSGA-II, in particular, was established as the most resorted strategy for obtaining a better spread of solutions and convergence than other multi-objective evolutionary algorithms (MOEAs) [95,118,119], which explains its selection for the present research.

GA's solution generation mechanisms [87,101,120–123] are modelled on Darwin's evolutionist theory of the survival of the fittest and natural selection mechanisms [124], where organisms gradually self-modify to produce generations better adapted to their environment and become dominant in their population [120]. For a comprehensive background on the Pareto-based optimisation concept, GA, and MOO, the interested reader can refer to [83].

Table 3 lists the calibration NSGA-II settings. The input parameters with most impact on computational burden and reliability of GA are the population size and the stopping criterion.

- **A reliable population size** ranges from 2-6 times the decision variables [105,109,111,125–130]. Thus, it was set at 20, i.e. four times the parameters. Values below this threshold could possibly affect the calibration end result by narrowing the solution sets [101,131] while values above it would increase convergence time without benefiting the solution finding process [132].
- **The maximum number of generations** (g_{MAX}) was used as the stopping criterion, i.e. GA stops searching after the maximum number of iterations that it is set to run for, due to being the most resorted to in building retrofit GA-based optimisation [83]. No official recommendations exist for the g_{MAX}. Moreover, given the broad range labelled as robust in the literature, i.e. between 10-200 generations [105,109,111,126,127,129,130,133], this research determined the g_{MAX} value though numerical tests assessing the trade-off between computational burden and reliability. The authors investigated a range from 10 (minimum value found in the literature [83]) to 200 (EA default settings) and examined whether the solutions remained unchanged beyond a specific number of generations. While the improvement was clear from 140 to 150 generations, it was minimal from 150 onwards, with near overlap of the last two generations (see Appendix B). Thusly, 150 generations were adopted for the calibration.
- **The genetic operators** were tuned according to the most used values in the literature, which stand between 40-100 % and 5-40 %, for crossover and mutation, respectively [83], so as to avoid loss of population diversity and premature convergence.

Table 3. Genetic settings for the optimisation-based calibration

GA Settings		**Values**
Exploration strategy	NSGA-II	
Population	Initial sampling size	20
Operators	Crossover rate (%)	100
	Mutation rate (%)	20
	Tournament size	2
Termination criterion	Maximum generations	150

Figure 3 further details the technical calibration process, and the interlocking of the different pieces of the process.

2.4.3. Validation and solution ranking

The selection of the Pareto front's best solution is referred to as the multi-criteria decision-making (MCDM) and can be conducted by means such as threshold compliance and the Utopia Point Method [84,111]. Here, a two-tier validation approach was developed for increased robustness, based on monitored indoor air temperature (12 weeks), surface temperature (72 hours), and relative humidity (12 weeks). It firstly entailed contrasting the Pareto-optimal solutions with objective function, i.e. MAE and RMSE, accuracy thresholds and secondly measuring the optimal solutions against the

analysis of residuals frequency (Fi), i.e. the difference between measured and simulated data, thresholds. The thresholds were adopted according to the most recent recommendations on dynamic hygrothermal historical building model validation [47]. A two-level validation process allows validation at different levels, as one RMSE and MAE value is obtained per solution, while Fi takes place for each time step (15 minutes). Specifically, as per [47], a model is considered validated when the MAE and RMSE values are within the ≤ 1 ºC/5 % (LV1) or ≤ 2 ºC/10 % (LV2) and when Fi ≥ 95 % of the overall dataset is within ± 1 ºC/5 % (LV1) or ± 2 ºC/10 % (LV2) intervals for T_a, T_s, and RH. Although an additional validating humidity parameter, such as humidity ratio or specific humidity, would have been desirable, the data were unavailable, which was acknowledged in the study limitations.

Subsequently, in a second step, Compromise Programming (CP) was implemented as a MCDM method for the validated solutions [134,135]. Through this method, the best solution is the closest to the ideal or Utopian point [126] that minimises both objective functions. For this purpose, a distance function considering the path from the nodes to the goal must be analysed. Here the Chebyshev distance function was adopted for performing superiorly to other approaches [136]. The CP problem definition thus aimed at minimising the Chebyshev distance, as follows:

$$\alpha_j \geq \left(\frac{\left|Z_j^* - Z_j(x)\right|}{\left|Z_j^* - Z_{*j}\right|}\right) * \left(p_j\right)$$

Where α_j is the Chebyshev distance, $Z_j\ (x)$ is the objective function, Z_j is the Utopian point which represents the ideal minimum solution, Z_j is the Nadir point (anti-ideal) of the jth objective, and p_j is the corresponding weight factor.

3. Results

3.1. U-value *in situ* measurements and standard assumptions

The results from the *in situ* experimental measurement of the U-values averaged 1.273 W/m^2.K for the external walls, bettering their theoretical average performance calculated based on the Portuguese traditional construction systems handbook [73] at 1.32 W/m^2.K. This high thermal transmittance value is in line with historical solid uninsulated walls, as is the lower *in situ* findings versus the calculated values. The baseline input data for modelling the external walls were based on the *in situ* measurements while the U-values from the remaining envelope were set according to the calculations from the traditional construction handbook [73] and ISO 10456. It would have been interesting to extend the external walls' U-value measurement to the entire envelopes, for the comprehensive model characterisation and comparison with theoretical values, which is acknowledged in the limitations section of this paper.

3.1. Parameter screening

Natural and mechanical ventilation model: The plot of the mean value and standard deviation obtained in the SA, suggested that the top five parameters influencing the MAE and RMSE regarding Ta were: the roof U-value, the

miscellaneous loads, airtightness, external wall U-value, and partition wall U-value (see Fig. 4.), with the first two clearly standing out. The parametric sensitivity to the MAE and RMSE globally followed the same trend, with slight differences

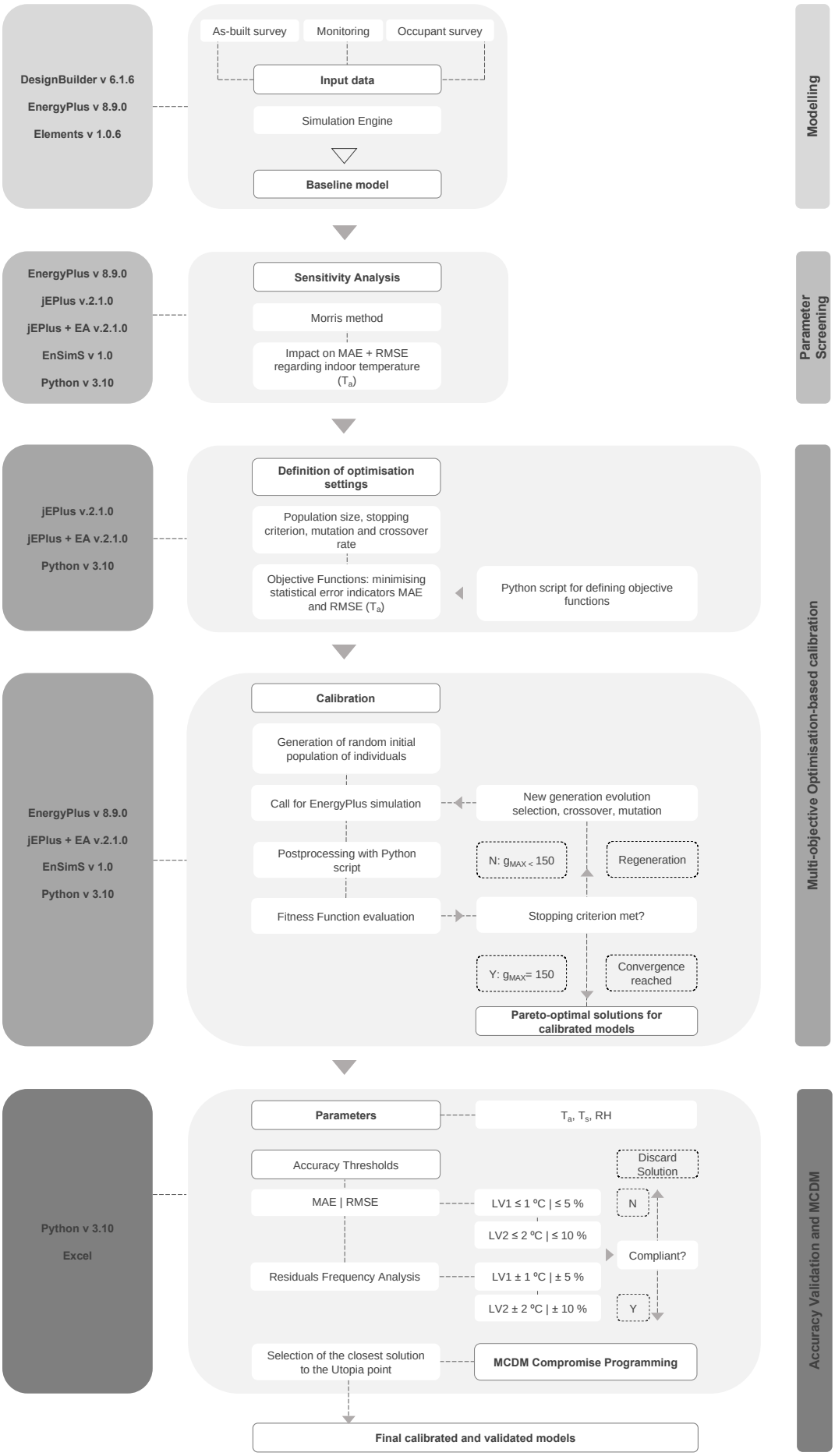

Fig. 3. Technical process for the calibration and validation of the vernacular case study models.

that did not impact the sensitivity ranking. That the roof thermal transmittance was the top influencing parameter was aligned with the authors' expectations given its extremely high theoretical U-value. Furthermore, it could be inferred that this feature would be key, not only for calibrating but also for future retrofit decision-making. That the internal miscellaneous gains from equipment had more impact than the external and partition walls thermal transmittance was a surprising finding, yet, previous research has reported it as the leading influencing parameter accounting for uncertainties regarding thermal comfort [137]. Airtightness ranked within the top effects, and the authors would expect the final calibration value to exceed the literature-based baseline. Lastly, the walls' thermal transmittance is a well-known influencing factor on the T_a and thermal comfort, all the more so in uninsulated heritage.

Electric heating model: the five parameters bearing the most influence on the MAE and RMSE regarding T_a were quite similar to the summer model, i.e. the roof U-value, the miscellaneous loads, airtightness, external wall U-value, and the linear thermal bridging (see Fig. 4.). In this case, the influence of the first three parameters is noteworthy. The need to optimise the linear thermal bridging parameters (Psi values) for the winter model is coherent due to being one of the weaknesses of the case studies. For this model, the solar absorptance-related inputs have negligible effects which may be explained by the season's different solar radiation. Please find the Morris method representation in the Appendix A.

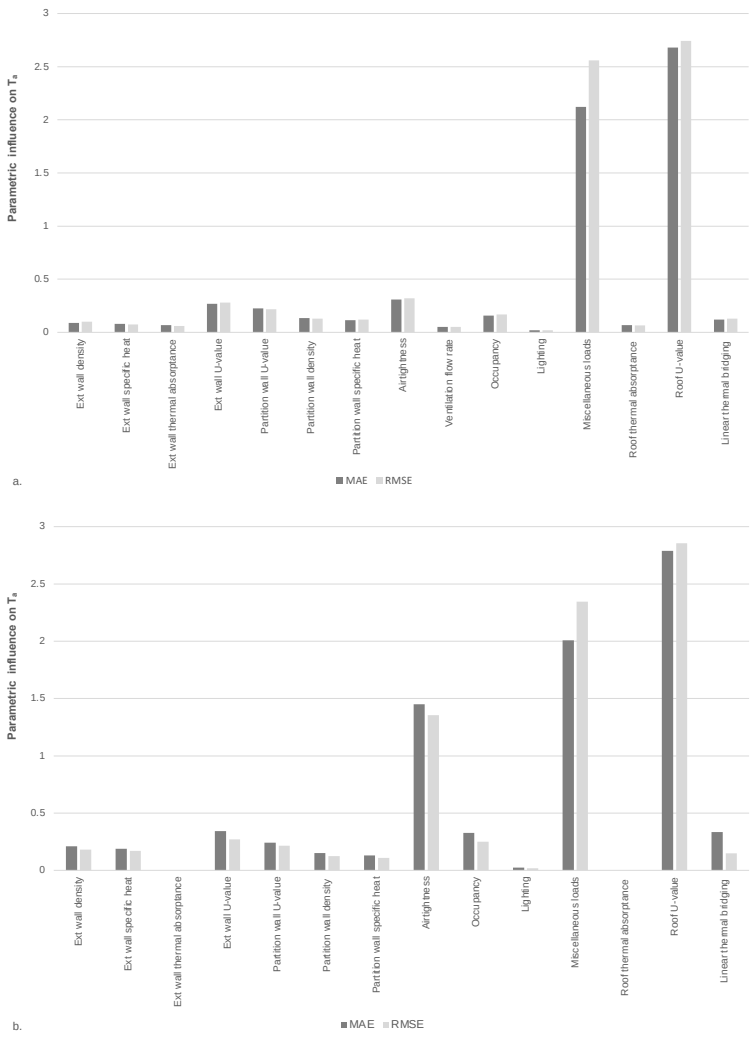

Fig. 4. Elementary effects on the MAE and RMSE of the average indoor air temperature (T_a) for the natural and mechanical ventilation model (a) and the electric heating model (b).

3.2. Model hygrothermal calibration

The SA revealed that the top influential parameters were the roof U-value, miscellaneous gains, airtightness, external and partition wall U-value, and linear thermal bridging. Since applying brute force search is infeasible from a time perspective, i.e. requiring 28.3544 years to achieve completion, a GA-based calibration was chosen as a suitable alternative to solve this MOO problem.

The above-mentioned parameters were then calibrated for each model, with NSGA-II needing only 1144 and 1129 simulations, in the winter and summer models respectively, to find the best solutions, and taking three hours in a PC with an Intel Core i5 processor 430M (2,27 GHz) and 6 GB of RAM. The scatter plot in Fig. 5 displays the NSGA-II optimisation where the best and feasible solutions (points) for simultaneously minimising the targets are provided. The red points are Pareto-optimal featuring the parameter set with the best trade-off values between both targets found by the GA. The Pareto frontier composed of nine and six optimal solutions for the summer and winter models, respectively, is displayed in the Appendix C.

As for the summer model, all nine best GA-found solutions radically reduced the RMSE value down to 0.0734, i.e. by 95 %, and the MAE to a range between 0.29 and 0.30, decreasing by around 78 %, with solution 1 (S1) offering the lowest MAE value. Nearly all input parameters set to be calibrated also exhibit a decrement regarding their baseline values. Specifically, the roof U-value improved by 25 % in all Pareto-optimal solutions, at 2.5 W/m^2.K, a value aligned with its uninsulated and heat infiltration characteristics. The miscellaneous loads are also optimised at a lower value, i.e. 10 W/m^2, in all six solutions. By the same token, all solutions diminished the external and partition wall U-value when compared to the *in situ*-measured value: 1.27 to 1.00 W/m^2.K. However, and as expected, the airtightness and linear thermal bridging increased to be more akin to the actual one. The airtightness, in particular, suggested at 1.85 ac/h by the best solutions, more than doubles its baseline value (0.8 ac/h). Even though the maximum range value was set based on the technical literature, it is possible that, due to the case studies' use patterns, this might even be exceeded.

Regarding the winter model, all six optimal solutions significantly reduced the statistical error indicators RMSE and MAE, with S1 and S2 reducing RMSE by more than 50 % and S5 and S6 reducing MAE by 54 %. The parameters set to be calibrated were overall reduced, with the external wall and roof U-value, miscellaneous loads, airtightness, and linear thermal bridging being parallel to the summer model. The values found for the partition wall, however, range between 0.9 and 1.23 W/m^2.K, slightly exceeding the baseline data at their upper limit.

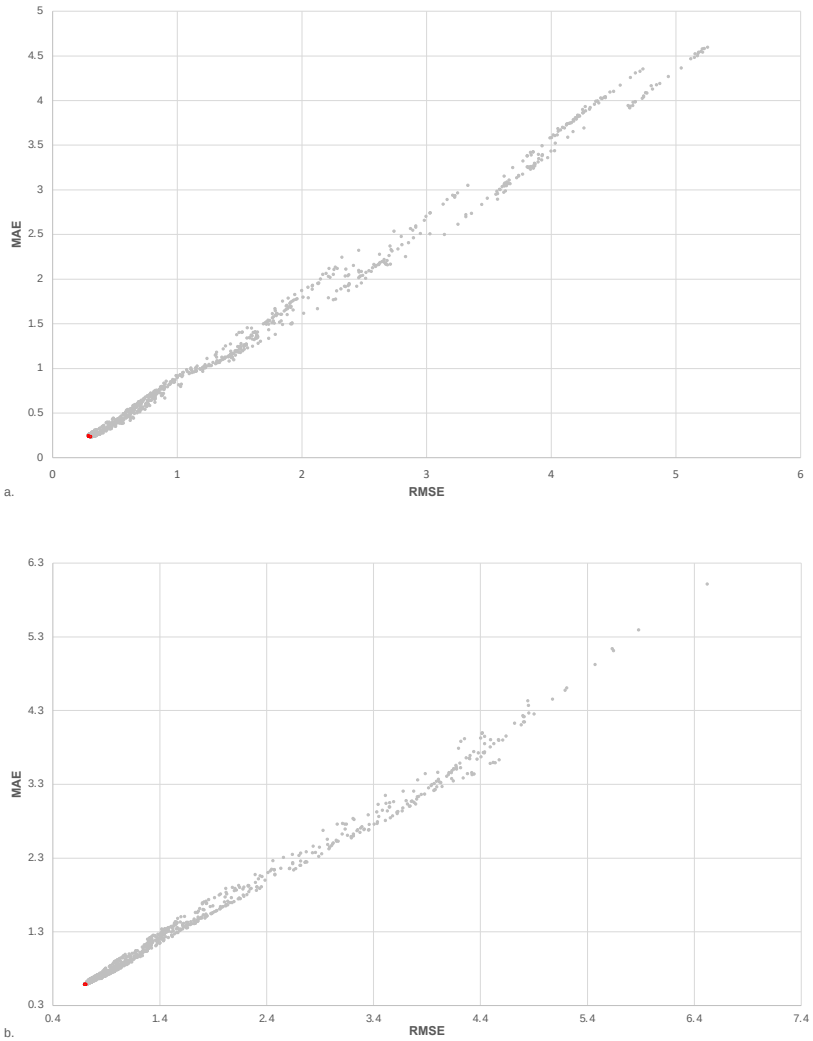

Fig. 5. Scatter plot of the GA optimisation output from jEPlus + EA for the summer (a) and winter (b) models. Red: Pareto-optimal points; grey: feasible points.

3.3. Model hygrothermal validation

Table 4 displays the results from the models' validation stage through the RMSE, MAE, and analysis of the frequency of residuals thresholds, regarding the indoor air temperature, surface temperature, and relative humidity.

For the winter model, while all Pareto-optimal solutions complied with LV1 threshold for MAE and RMSE concerning T_a, at the RH level, compliance is only observed for the LV2 accuracy range. Thus, based on the objective function thresholds all optimal solutions found by NSGA-II would be validated, with T_a holding better accuracy regarding measured data. Out of these, only one solution (S3) complied with Fi's LV2 thresholds (≥ 95 % of residuals, ± 2 ºC). While Fi reveals a better outcome for T_{as} than for RH (100 % within threshold), both parameters failed to qualify for LV1 match (≥ 95% of residuals, ± 1 ºC), ranging between 83 % for T_{as} to 78 % for RH (see Appendix D2). On the basis of a single optimal solution being validated, the decision-making process for the winter model would end at this stage by calibrating the model according to the features of S3 (Appendix C). This translated into an accuracy improvement of 51

% and 54 % for the RMSE and MAE, respectively. Airtightness (P8) was the parameter undergoing the biggest adjustment, while the partition wall specific heat (P7) exhibited only minor modification. Said accuracy improvement can also be detected in Fig. 7., where a representative week of the calibrated T_{as} is contrasted with the baseline and measured T_{as}, and in the dispersion chart representing the correlation between the measured T_{as} versus baseline (grey dots) and calibrated (orange dots) data. The blue line depicts the perfect fit of measured versus measured, and, thus, the closer to that reference axis the highest the accuracy. The calibrated dot cloud is clearly more centred around the reference axis and shows a lesser degree of dispersion, bettering the performance of the baseline simulation.

For the summer model, all Pareto-optimal solutions largely qualify for LV1 accuracy for MAE and RMSE concerning T_a and T_s. Analogously to the winter model, at the RH level, compliance is only observed for the LV2 accuracy range, albeit significantly bettering their winter counterpart, with RH RMSE and MAE lowering by 60 % and over 50 % on average. As for the Fi in the following step, conversely to the winter model, all solutions complied with the LV2 threshold, with T_a and T_s exhibiting the most favourable residuals distribution (100 % within the threshold) and also complying with LV1 match threshold. As in the winter model, RH displays less concordance than the latter parameters, with the highest percentage distribution being 78 and 98 for LV1 and LV2 thresholds, respectively (See Appendix D1). The MCDM process thus proceeded to the Compromise Programming stage to determine the closest solution to the Utopia Point, as can be seen in the Appendix E. The results showed that S4 exhibited the shortest Chebyshev distance, followed by S5, with S1 and S9 displaying the worst values. The model was then calibrated per the features of S4, which resulted in a noteworthy accuracy improvement of 80 % for the RMSE and 81 % in terms of the MAE. Airtightness (P8) was anew the most altered parameter, by 131 % in regard to the BM, while the calibrated roof thermal absorptance value (P13) was akin to the baseline. The difference between the measured, baseline, and calibrated data can be observed for a representative week in Figures 6 and 7, evidencing the accuracy enhancement of the calibrated data regarding the BM.

Table 4. Frequency of residuals contrasted with the validation thresholds for the summer and winter models, respectively.

	T_a Fi		RH Fi		T_s Fi		T_a RMSE		T_a MAE		RH RMSE		RH MAE		T_s RMSE		T_s MAE	
	LV1	**LV2**	**LV1**	**LV2**	**LV1**	**LV2**	**LV1**	**LV2**	**LV1**	**LV2**	**LV1**	**LV2**	**LV1**	**LV2**	**LV1**	**LV2**	**LV1**	**LV2**
SUMMER																		
S1	100%	100%	77%	97%	95%	100%	0.29		0.25		5.92		4.54		0.81		0.64	
S2	100%	100%	77%	97%	95%	100%	0.29		0.24		5.86		4.51		0.82		0.65	
S3	100%	100%	77%	97%	95%	100%	0.29		0.24		5.85		4.50		0.82		0.65	
S4	**100%**	**100%**	**78%**	**98%**	**96%**	**100%**	**0.29**		**0.24**		**5.83**		**4.48**		**0.80**		**0.63**	
S5	100%	100%	75%	98%	96%	100%	0.29		0.24		5.82		4.48		0.80		0.63	
S6	100%	100%	78%	98%	96%	100%	0.30		0.24		5.79		4.46		0.79		0.62	
S7	100%	100%	74%	97%	96%	100%	0.30		0.24		5.77		4.45		0.81		0.64	
S8	100%	100%	74%	98%	96%	100%	0.30		0.24		5.77		4.43		0.89		0.63	
S9	100%	100%	75%	97%	96%	100%	0.31		0.24		5.76		4.44		0.81		0.64	
VT	± 1 ºC	± 2 ºC	± 5 %	± 10 %	± 1 ºC	± 2 ºC	≤ 1 ºC	≤ 2 ºC	≤ 1 ºC	≤ 2 ºC	≤ 5 %	≤ 10 %	≤ 5 %	≤ 10 %	≤ 1 ºC	≤ 2 ºC	≤ 1 ºC	≤ 2 ºC
WINTER																		
S1	83%	100%	74%	93%	-	-	0.70		0.59		9.48		7.28		-		-	
S2	83%	100%	75%	94%	-	-	0.70		0.59		9.43		7.22		-		-	
S3	**83%**	**100%**	**78%**	**95%**	**-**	**-**	**0.70**		**0.59**		**9.20**		**6.83**		**-**		**-**	
S4	83%	100%	77%	94%	-	-	0.71		0.59		9.27		7.00		-		-	
S5	83%	100%	72%	92%	-	-	0.71		0.59		9.77		7.65		-		-	
S6	83%	100%	74%	93%	-	-	0,71		0.59		9.48		7.28		-		-	
VT	± 1 ºC	± 2 ºC	± 5 %	± 10 %	± 1 ºC	± 2 ºC	≤ 1 ºC	≤ 2 ºC	≤ 1 ºC	≤ 2 ºC	≤ 5 %	≤ 10 %	≤ 5 %	≤ 10 %	≤ 1 ºC	≤ 2 ºC	≤ 1 ºC	≤ 2 ºC

T_a Fi: Indoor Temperature Residuals Frequency; RH Fi: Relative Humidity Residuals Frequency; T_s Fi: Surface Temperature Residuals Frequency; T_a RMSE: Indoor Temperature RMSE; T_a MAE: Indoor Temperature MAE; RH RMSE: Relative Humidity RMSE; RH MAE: Relative Humidity MAE; T_s RMSE: Surface Temperature RMSE; T_s MAE: Surface Temperature MAE; VT: Validation Threshold; LV1: Level 1; LV2: Level 2.

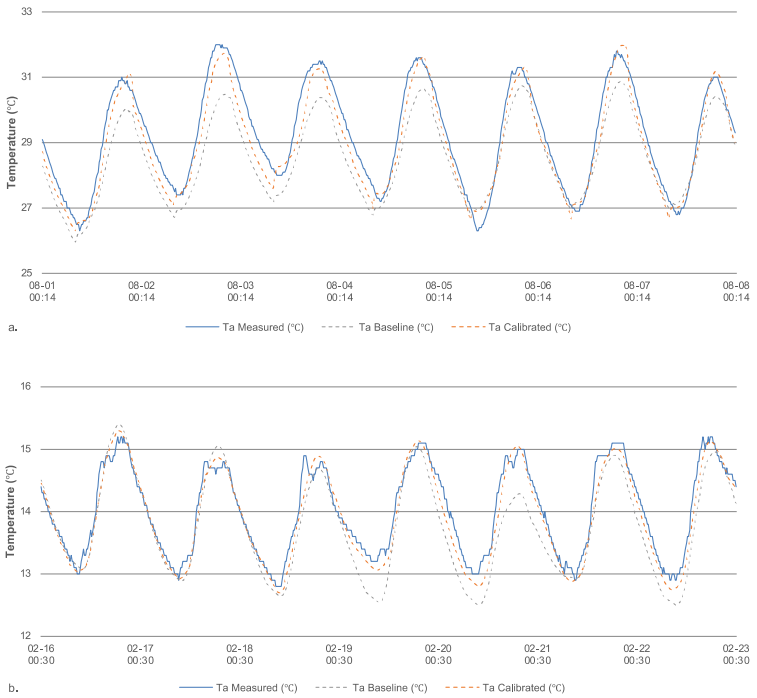

Fig. 6. Representative week of measured versus baseline and calibrated indoor air temperature, for the summer (a) and winter (b) models. The representative summer week (1st-8th of August) was chosen for being the hottest week of the monitoring while the winter representative week (16th-23th of February) was selected over the coldest week due to an atypical weather event.

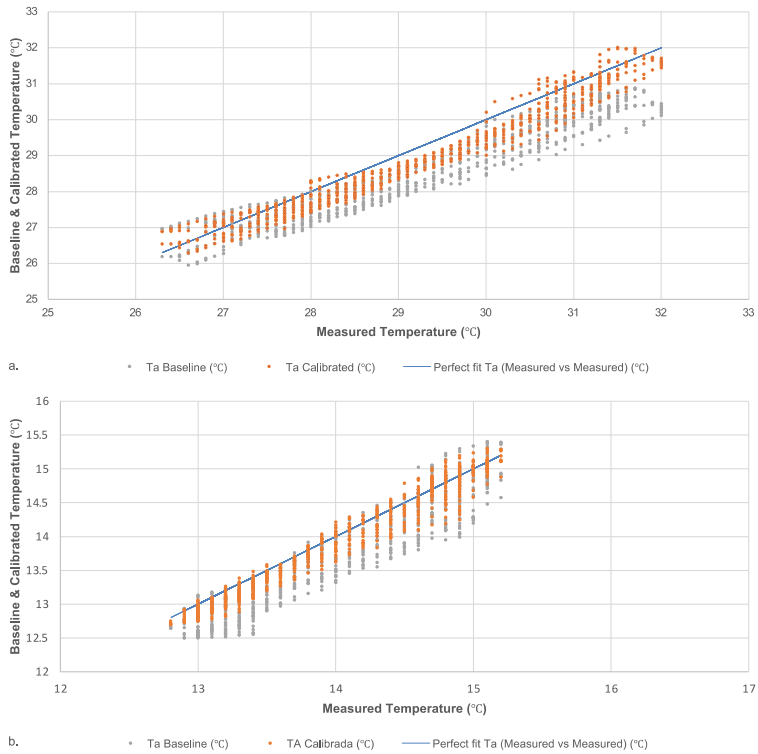

Fig. 7. Dispersion graphic: measured indoor air temperature versus baseline and calibrated data, for the summer (a) and winter (b) models.

4. Conclusion

4.1. Summary of main findings

This paper set forth a methodology for the calibration and validation of vernacular case study models, with the **intent of building a common framework for counteracting the high degree of dispersion amongst vernacular modelling studies** and foster more robust research. **It aimed to, for the first time, address hygrothermal calibration in vernacular dwellings with heritage-adequate error indexes coupled with a two-tier validation scheme.** Additionally, it strove to meet the following criteria: highest degree of accuracy alongside time-efficiency, baseline data based on on-site data collection, and transparency regarding the calibration and validation parameters, period, and thresholds used. Following the *in situ* data collection that encompassed the as-built survey, environmental and thermophysical monitoring, and occupant surveying of 22 vernacular dwellings in Southern Portugal, the hygrothermal modelling method was composed of three main steps: **the sensitivity analysis, the optimisation-based calibration, and the validation and MCDM.**

- **Sensitivity analysis:** conducted to ascertain the model's parametric effect on the statistical error indicators MAE and RMSE regarding indoor air temperature. The top influential parameters were found to be the roof U-value, miscellaneous gains, airtightness, external and partition wall U-value, and linear thermal bridging.
- **Calibration:** a GA multi-objective optimisation-based calibration was implemented as an alternative to other time-consuming and infeasible search techniques, simultaneously minimising the objective functions of RMSE and MAE. NSGA-II found Pareto frontiers composed of nine and six optimal solutions for the summer and winter models, respectively, taking approximately three hours each. All optimal solutions significantly decreased the RMSE and MAE, especially in the summer model.
- **Validation:** three validating parameters (indoor air temperature, surface temperature, and relative humidity) were adopted. Based on the objective function thresholds all winter optimal solutions found by NSGA-II were validated, with T_a holding better accuracy regarding measured data. Yet, the subsequent validation step against the Fi thresholds revealed that only one winter optimal solution met the LV2 accuracy threshold, thus stopping the validation process with an accuracy improvement of 51 % and 54 % for the T_a RMSE and T_a MAE, respectively, and very strong correlation between the calibrated and the measured data. In the summer model, all optimal solutions were validated according to the RMSE and MAE LV1 threshold for T_a and T_s and LV2 for RH, bettering the validation results of the winter model. By the same token, all complied with Fi's LV2 thresholds, with T_a and T_s also qualifying for LV1 accuracy. MCDM was then conducted through Compromise Programming to determine the closest solution to the Utopia Point and calibrate the model accordingly, resulting in a noteworthy accuracy improvement of 80 % for the T_a RMSE and 81 % for T_a MAE.

The strong correlation found for both models between calibrated and measured values as well as the accuracy enhancement of the calibrated data regarding the BM obtained via the methodology developed, highlighted that it is not only possible but efficient to use GAs to obtain calibrated models of vernacular dwellings that robustly predict real building performance and can foster better decision-making for retrofitting heritage buildings.

4.2. Limitations of the study and suggestions for further work

Concerning the on-site measurements, it would have been interesting to extend the external walls' U-value measurement to the entire envelopes, for the comprehensive model characterisation and comparison with theoretical values. Nonetheless, the latter were sourced from a traditional buildings Portuguese handbook [73], with the intent of reducing the experimental-theoretical gap. The authors acknowledge that the exact location of the sensors was not investigated by means of thermography as suggested in ISO 6781:1983 [138] and it would be desirable to include it in future work. Nonetheless, the triple sensor scheme of the probe used aims at ensuring a result that is representative of the whole element as indicated in ISO 9869-1-2014 and compliant with ISO 6946:2017. Moreover, although not essential, had the technical means been available, it would have been desirable to use an additional validating humidity parameter. However, a double validation step was conducted for enhanced robustness using three validation parameters. Moreover, future research might consider getting further insight into the airtightness of these types of dwellings, encompassing blower-door testing and widening the upper airtightness range for the calibration process of the models.
Finally, future work is needed to extend this GA-based MOO calibration methodology to heritage retrofit decision-making, and specifically inhabited vernacular dwellings, targeting both thermal comfort and the quantification of conservation parameters. This could, perhaps, be achieved via the Analytic Hierarchy Process and the definition of heritage protection legislation as constraints in the MOO problem.

Declaration of Competing Interest

The authors declare that they have no known competing financial interests or personal relationships that could have appeared to influence the work reported in this paper.

Acknowledgements

This work was supported by the Foundation for Science and Technology (FCT) from the Portuguese Ministry for Science, Technology and Higher Education (Grant No.: SFRH/BD/95911/2013) and its financing programme POPH/FSE.

Appendix

Appendix A. Details of the *in situ* monitoring conducted.

	Parameter	Measurement length			Location of measurement	Standard complied with
		LT [(1)]	ST [(2)]	PIT [(3)]		
Thermal comfort	Air temperature	■			Living room, bedroom, outdoors	ISO 7726 [77], ASHRAE 55 [80]
	Relative humidity	■			Living room, bedroom, outdoors	ISO 7726, ASHRAE 55
	Mean radiant temperature		■		Living room	ISO 7243, ISO 7726, EN 27726
	Surface temperature		■		Living room/bedroom	-
	U-value		■		Living room/bedroom	ISO 9869-1:2014 [58], ISO 6946:2017 [59]
	Air velocity			■	Living room	ASHRAE 55, ISO 7726
Other	Indoor air quality			■	Living room	EN 15251 [65]
Environmental parameters	Illuminance			■	Living room, outdoors	EN 15251 EN 12464-1:2011 [66]
	Noise level			■	Living room, outdoors	EN 15251

[(1)] Long-term; [(2)] Short-term; [(3)] Point-in-time.

Appendix B. Morris method representation for summer (a) and Winter (b) models.

a.

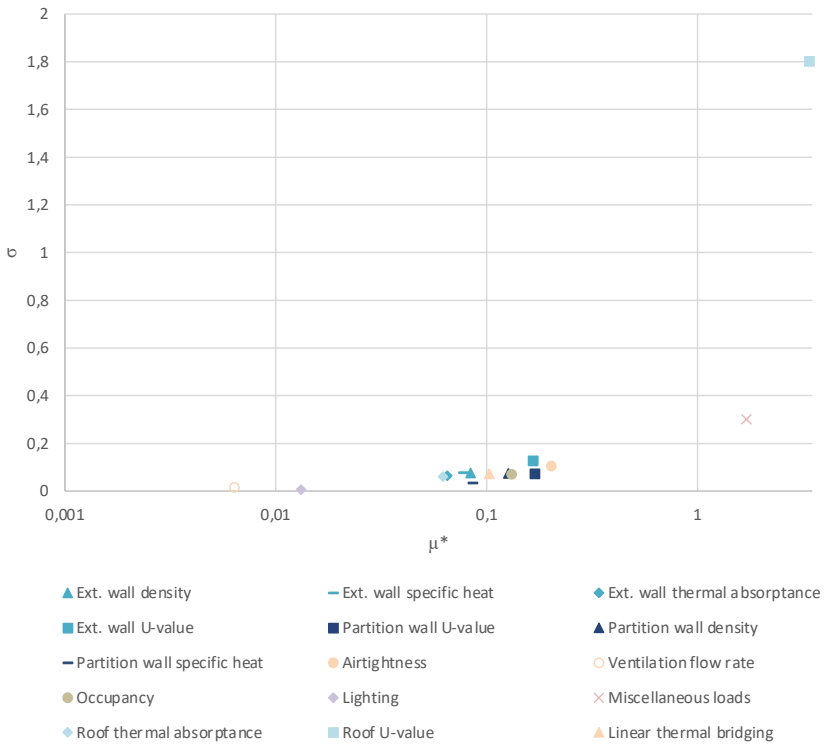

b.

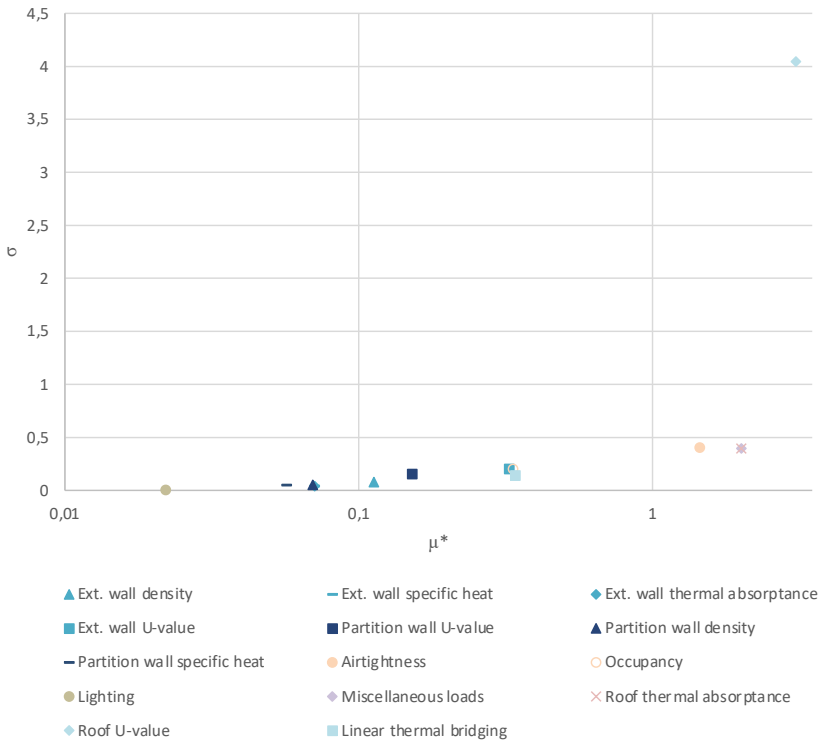

Appendix C. Pareto fronts resulting from the GA-based multi-objective optimisation for model calibration, in function of the number of maximum generations (g_{max}).

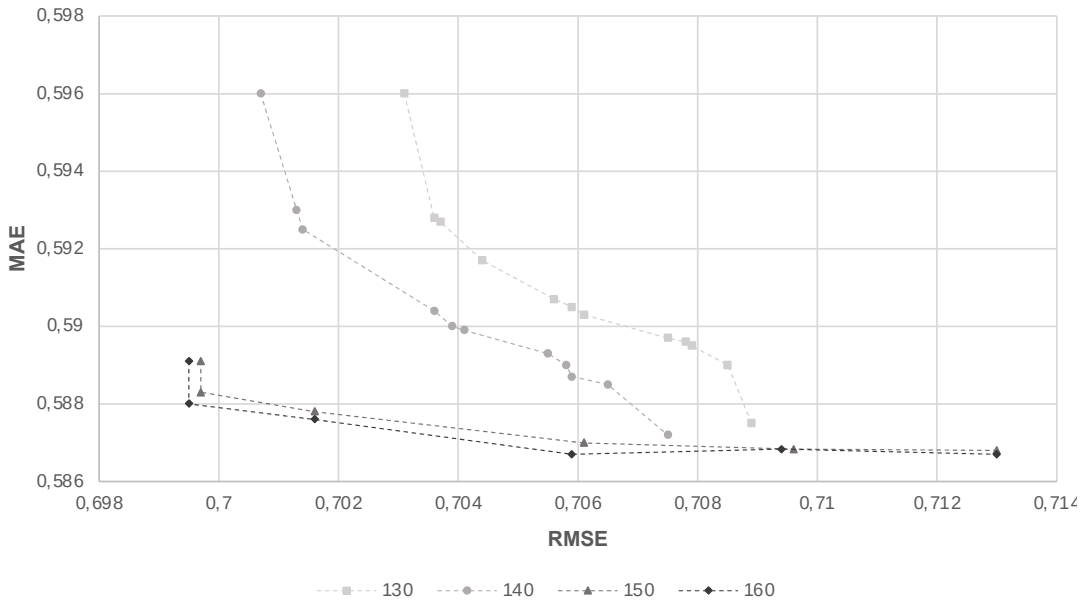

Appendix D. Features of the Pareto Front for the summer and winter models, respectively.

Solution	RMSE	MAE	P1	P2	P3	P4	P5	P6	P7	P8	P9	P10	P11	P12	P13	P14	P15
SUMMER																	
BM	1.4322279	1.2806087	1800	900	0.900	1.273	1.172	1800	900	0.800	0.096	1.000	7.190	17	0.900	3.130	2.500
S1	0.2866159	0.2461452	2100	999	0.860	1.000	0.900	2500	733	1.850	0.050	0.600	9.590	10	0.940	2.500	2.000
S2	0.2885968	0.2406363	2100	733	0.860	1.000	0.900	2500	733	1.850	0.050	0.600	9.590	10	0.700	2.500	2.000
S3	0.2896586	0.2394249	2500	600	0.940	1.000	0.900	2500	733	1.850	0.050	0.600	9.590	10	0.940	2.500	2.000
S4	**0.2905343**	**0.2380866**	**2500**	**733**	**0.780**	**1.000**	**0.900**	**2500**	**733**	**1.850**	**0.050**	**0.600**	**9.590**	**10**	**0.940**	**2.500**	**2.000**
% DIFF BM	**-80 %**	**-81 %**	**39 %**	**-19 %**	**-13 %**	**-21 %**	**-23 %**	**39 %**	**-19 %**	**131 %**	**-48 %**	**-40 %**	**33 %**	**-41 %**	**4 %**	**-20 %**	**-20 %**
S5	0.2910137	0.2377589	2100	866	0.700	1.000	0.900	2500	733	1.850	0.050	0.600	9.590	10	0.700	2.500	2.000
S6	0.3011555	0.2363003	2100	999	0.780	1.000	0.900	2100	733	1.850	0.050	0.600	9.590	10	0.780	2.500	2.000
S7	0.3024440	0.2362210	1300	999	0.860	1.000	0.900	2500	733	1.850	0.050	0.600	9.590	10	0.860	2.500	2.000
S8	0.3032757	0.2360333	1700	999	0.700	1.000	0.900	2500	733	1.850	0.050	0.600	9.590	10	0.780	2.500	2.000
S9	0.3053097	0.2360279	2100	600	0.780	1.000	0.900	2500	733	1.850	0.050	0.600	9.590	10	0.940	2.500	2.000
WINTER																	
BM	1.4322279	1.2806087	1800	900	0.900	1.273	1.172	1800	900	0.800	0.096	1.000	7.190	17	0.900	3.130	-
S1	0.6996679	0.5891419	1300	600	0.700	1.000	0.900	2100	866	1.850	0.050	0.600	9.590	10	0.700	2.500	-
S2	0.6997473	0.5882981	1300	600	0.700	1.000	1.233	2100	999	1.850	0.050	0.600	9.590	10	0.780	2.500	-
S3	**0.7016192**	**0.5875125**	**1300**	**600**	**0.700**	**1.000**	**1.233**	**2500**	**866**	**1.850**	**0.050**	**0.600**	**9.590**	**10**	**0.700**	**2.500**	**-**
% DIFF BM	**-51 %**	**-54 %**	**-28 %**	**-33 %**	**-22 %**	**-21 %**	**5 %**	**39 %**	**-4 %**	**131 %**	**-48 %**	**-40 %**	**33 %**	**-41 %**	**-22 %**	**-20 %**	**-**
S4	0.7061431	0.5870416	1300	600	0.700	1.000	1.233	2100	866	1.850	0.050	0.600	9.590	10	0.700	2.500	-
S5	0.7096275	0.5868355	1300	600	0.700	1.000	0.900	2500	866	1.850	0.050	0.600	9.590	10	0.700	2.500	-
S6	0,7129966	0.5868369	1300	600	0.700	1.000	1.400	2500	866	1.850	0.050	0.600	9.590	10	0.700	2.500	-

BM**:** Baseline Model; P1: External wall density; P2: External wall specific heat; P3: External wall thermal absorptance; P4: External wall U-value; P5: Partition wall U-value; P6: Partition wall density; P7: Partition wall specific heat; P8: Airtightness; P9: Occupancy; P10: Lighting; P11: Linear thermal bridging; P12: Miscellaneous loads; P13: Roof thermal absorptance; P14: Roof U-value; P15: Ventilation flow rate.

Appendix E1. Residuals frequency distribution for indoor air temperature, relative humidity, and surface temperature regarding the summer model (S4).

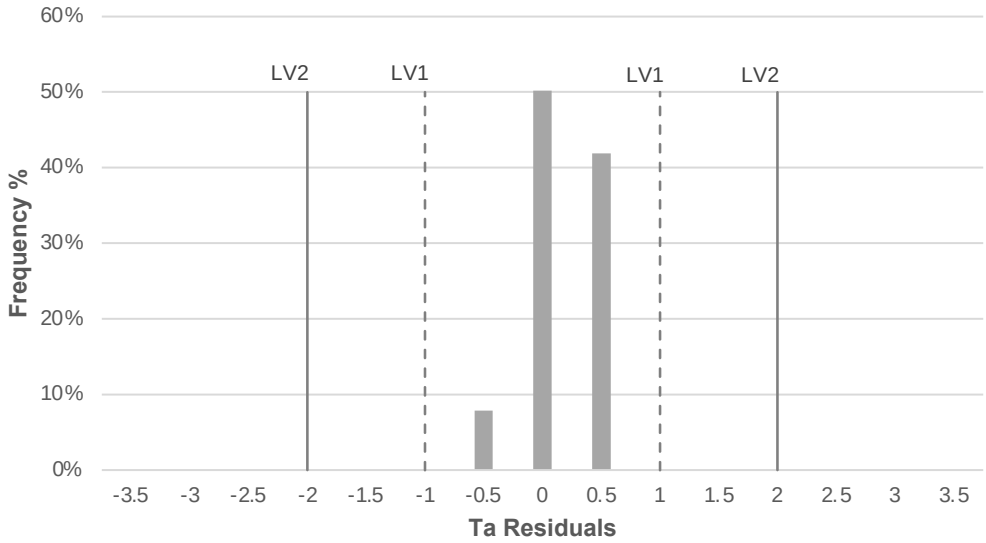

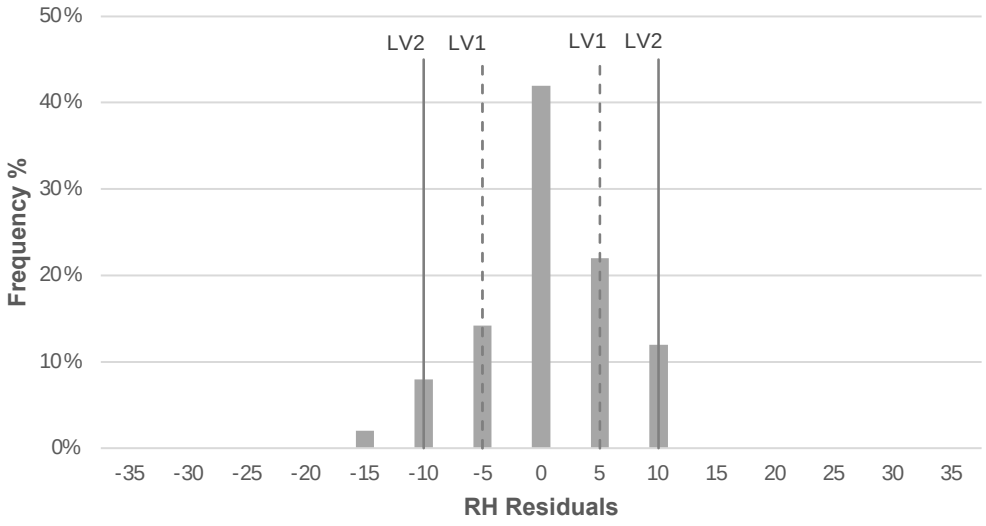

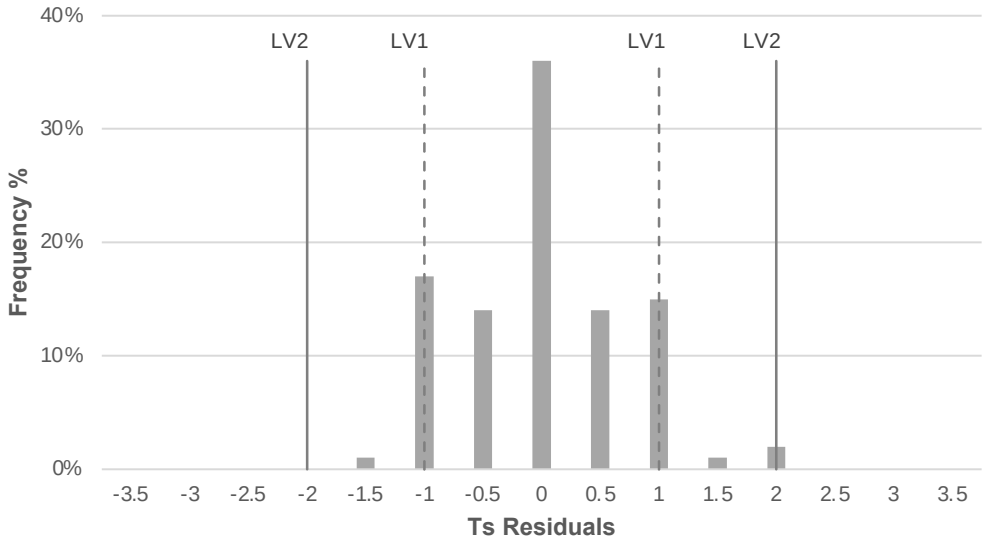

Appendix E2. Residuals frequency distribution for indoor air temperature and relative humidity regarding the winter model (S3).

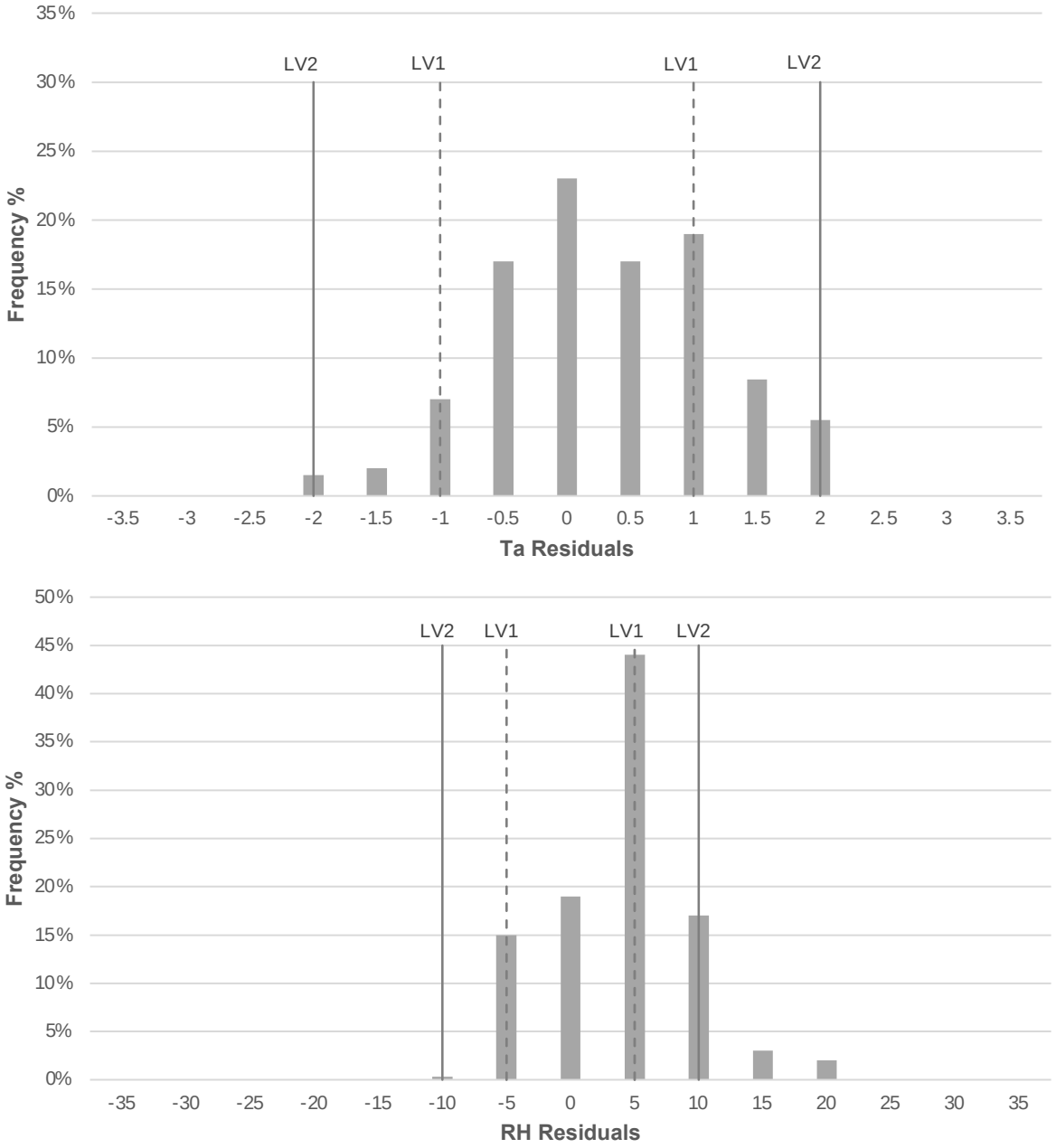

Appendix F. Illustration of the Pareto fronts with the Utopia and Nadir points, for the summer (a) and winter (b) models.

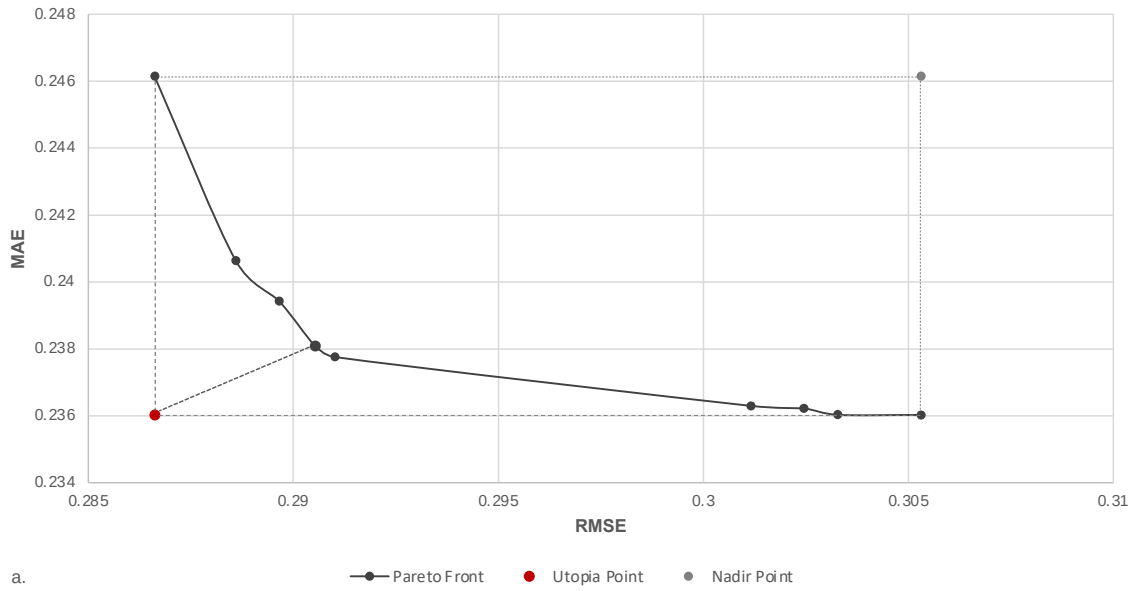

a.

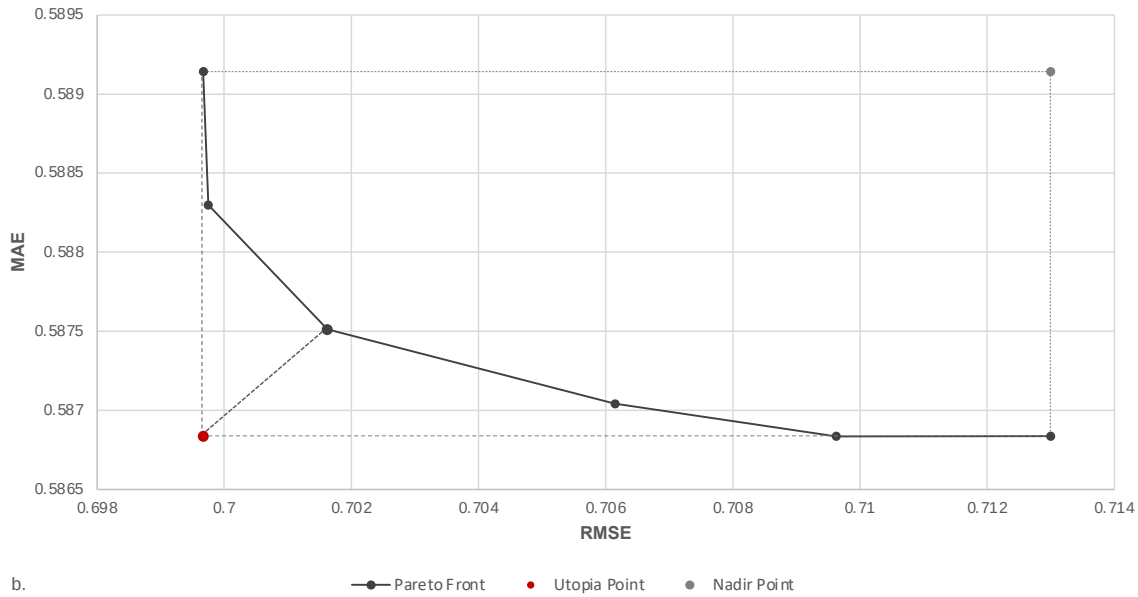

b.

References

[1] P. Oliver, Encyclopedia of Vernacular Architecture of the World, Cambridge University Press, Cambridge, 1997.

[2] P. Oliver, Dwellings: The Vernacular House Worldwide, Phaidon Press, 2013.

[3] G.G. Akkurt, N. Aste, J. Borderon, A. Buda, M. Calzolari, D. Chung, V. Costanzo, C. Del Pero, G. Evola, H.E. Huerto-Cardenas, F. Leonforte, A. Lo Faro, E. Lucchi, L. Marletta, F. Nocera, V. Pracchi, C. Turhan, Dynamic thermal and hygrometric simulation of historical buildings: Critical factors and possible solutions, Renew. Sustain. Energy Rev. 118 (2020) 109509. doi:10.1016/j.rser.2019.109509.

[4] I. Costa-Carrapiço, J. Neila González, R. Raslan, C. Sánchez-Guevara Sánchez, Understanding the Challenges of Determining Thermal Comfort in Vernacular Dwellings: A Meta-Analysis, Available SSRN Https//Ssrn.Com/Abstract=3944617. (2021).

[5] F. Roberti, U.F. Oberegger, A. Gasparella, Calibrating historic building energy models to hourly indoor air and surface temperatures: Methodology and case study, Energy Build. 108 (2015) 236–243. doi:10.1016/j.enbuild.2015.09.010.

[6] J. Zhu, L. Tong, R. Li, J. Yang, H. Li, Annual thermal performance analysis of underground cave dwellings based on climate responsive design, Renew. Energy. 145 (2020) 1633–1646. doi:10.1016/j.renene.2019.07.056.

[7] M. Zune, L. Rodrigues, M. Gillott, Vernacular passive design in Myanmar housing for thermal comfort, Sustain. Cities Soc. 54 (2020) 101992. doi:10.1016/j.scs.2019.101992.

[8] G. Yao, D. Han, L. Zhang, Z. Duan, The Thermal Performance of Chinese Vernacular Skywell Dwellings, Adv. Civ. Eng. 2021 (2021). doi:10.1155/2021/6666701.

[9] M. Tahsildoost, Z.S. Zomorodian, Energy, carbon, and cost analysis of rural housing retrofit in different climates, J. Build. Eng. 30 (2020) 101277. doi:10.1016/j.jobe.2020.101277.

[10] K. Henna, A. Saifudeen, M. Mani, Resilience of vernacular and modernising dwellings in three climatic zones to climate change, Sci. Rep. 11 (2021) 1–14. doi:10.1038/s41598-021-87772-0.

[11] G. Tsovoodavaa, I. Kistelegdi, Comparative analysis for traditional yurts using thermal dynamic simulations in Mongolian climate, Pollack Period. 14 (2019) 97–108. doi:10.1556/606.2019.14.2.9.

[12] A. Michael, C. Heracleous, S. Thravalou, M. Philokyprou, Lighting performance of urban vernacular architecture in the East-Mediterranean area: Field study and simulation analysis, Indoor Built Environ. 26 (2017) 471–487. doi:10.1177/1420326X15621613.

[13] A. Heidari, S. Sahebzadeh, Z. Dalvand, Natural ventilation in vernacular architecture of Sistan, Iran; Classification and CFD study of compound rooms, Sustain. 9 (2017). doi:10.3390/su9061048.

[14] A. Kaihoul, L. Sriti, K. Amraoui, S. Di Turi, F. Ruggiero, The effect of climate-responsive design on thermal and energy performance: A simulation based study in the hot-dry Algerian South region, J. Build. Eng. 43 (2021). doi:10.1016/j.jobe.2021.103023.

[15] V. Shastry, M. Mani, R. Tenorio, Impacts of modern transitions on thermal comfort in vernacular dwellings in warm-humid climate of Sugganahalli (India), Indoor Built Environ. 23 (2014) 543–564. doi:10.1177/1420326X12461801.

[16] F. Bougiatioti, A. Oikonomou, Architectural characteristics and environmental performance of byzantine houses and streets, Build. Environ. 170 (2020) 106605. doi:10.1016/j.buildenv.2019.106605.

[17] F. Chi, I. Borys, L. Jin, Z. Zhu, D. Bart, The strategies and effectiveness of climate adaptation for the thousand pillars dwelling based on passive elements and passive spaces, Energy Build. 183 (2019) 17–44. doi:10.1016/j.enbuild.2018.10.029.

[18] A. Mohammadi, M.R. Saghafi, M. Tahbaz, F. Nasrollahi, The study of climate-responsive solutions in traditional dwellings of Bushehr City in Southern Iran, J. Build. Eng. 16 (2018) 169–183. doi:10.1016/j.jobe.2017.12.014.

[19] X. Juan, L. Ziliang, G. Weijun, Y. Mengsheng, S. Menglong, The comparative study on the climate adaptability based on indoor physical environment of traditional dwelling in Qinba mountainous areas, China, Energy Build. 197 (2019) 140–155. doi:10.1016/j.enbuild.2019.05.045.

[20] H. Sözer, S. Bekele, Evaluation of innovative sustainable design techniques from traditional architecture: a case study for the cold dry climatic region in Turkey, Archit. Sci. Rev. 61 (2018) 143–155. doi:10.1080/00038628.2018.1457509.

[21] C. Kabre, Sustainable Greek traditional dwellings of Cyclades, Archit. Sci. Rev. 59 (2016) 81–90. doi:10.1080/00038628.2015.1082901.

[22] A. Udaykumar, E. Rajasekar, R. Venkateswaran, Thermal comfort characteristics in naturally ventilated, residential apartments in a hot-dry climate of India, Indoor Built Environ. 24 (2015) 101–115. doi:10.1177/1420326X13504120.

[23] L. Gazquez, F. Fernández, J. Cejudo, A Comparison of Traditional and Contemporary Social Houses in Catarmarca (Argentina). Comfort Conditions and Life Cycle Assessment, 82 (2022).

[24] E. Genova, G. Fatta, C. Vinci, The Recurrent Characteristics of Historic Buildings as a Support to Improve their Energy Performances: The Case Study of Palermo, Energy Procedia. 111 (2017) 452–461. doi:10.1016/j.egypro.2017.03.207.

[25] B. Ozarisoy, H. Altan, Systematic literature review of bioclimatic design elements: Theories, methodologies and cases in the South-eastern Mediterranean climate, Energy Build. 250 (2021). doi:10.1016/j.enbuild.2021.111281.

[26] B.A. Timur, T. Başaran, B. İpekoğlu, Thermal retrofitting for sustainable use of traditional dwellings in

Mediterranean climate of southwestern Anatolia, Energy Build. 256 (2022). doi:10.1016/j.enbuild.2021.111712.

[27] A. Egusquiza, S. Ginestet, J.C. Espada, I. Flores-Abascal, C. Garcia-Gafaro, C. Giraldo-Soto, S. Claude, G. Escadeillas, Co-creation of local eco-rehabilitation strategies for energy improvement of historic urban areas, Renew. Sustain. Energy Rev. 135 (2021). doi:10.1016/j.rser.2020.110332.

[28] B. Montalbán Pozas, F.J. Neila González, Hygrothermal behaviour and thermal comfort of the vernacular housings in the Jerte Valley (Central System, Spain), Energy Build. 130 (2016) 219–227. doi:10.1016/j.enbuild.2016.08.045.

[29] J. Zhu, P. Nie, R. Li, L. Tong, X. Zhao, Climate responsive characteristics of cliff-side cave dwellings in cold area of China, Energy Procedia. 158 (2019) 2731–2736. doi:10.1016/j.egypro.2019.02.030.

[30] B. Widera, Comparative analysis of user comfort and thermal performance of six types of vernacular dwellings as the first step towards climate resilient, sustainable and bioclimatic architecture in western sub-Saharan Africa, Renew. Sustain. Energy Rev. 140 (2021) 110736. doi:10.1016/j.rser.2021.110736.

[31] J. Gupta, M. Chakraborty, Perimeter-area ratios and thermal discomfort due to excess heat in rural mud architecture of jharkhand: A study through simulation and temperature measurements in composite climate, Int. J. Appl. Eng. Res. 10 (2015) 17503–17518. doi:10.37622/ijaer/10.7.2015.17503-17518.

[32] P. Stefanizzi, I. Fato, S. Di Turi, Energy and environmental performance of trullo stone building. An experimental and numerical survey, Int. J. Heat Technol. 34 (2016) S396–S402. doi:10.18280/ijht.34S229.

[33] J. Alabid, A. Taki, Optimising residential courtyard in terms of social and environmental performance for Ghadames Housing, Libya, Proc. 33rd PLEA Int. Conf. Des. to Thrive, PLEA 2017. 3 (2017) 4998–5005.

[34] S. Gou, Z. Li, Q. Zhao, V.M. Nik, J.L. Scartezzini, Climate responsive strategies of traditional dwellings located in an ancient village in hot summer and cold winter region of China, Build. Environ. 86 (2015) 151–165. doi:10.1016/j.buildenv.2014.12.003.

[35] X. Zhao, P. Nie, J. Zhu, L. Tong, Y. Liu, Evaluation of thermal environments for cliff-side cave dwellings in cold region of China, Renew. Energy. 158 (2020) 154–166. doi:10.1016/j.renene.2020.05.128.

[36] V. Shastry, M. Mani, R. Tenorio, Evaluating thermal-comfort and building climatic-response in warm-humid climates for vernacular dwellings in Suggenhalli (India), Archit. Sci. Rev. 59 (2016) 12. doi:10.1080/00038628.2014.971701.

[37] P. Stefanizzi, P. Bari, P. Bari, P. Bari, P. Stefanizzi, I. Fato, F. Ladisa, S. Di, T. Politecnico, Energy and environmental performance of Trullo stone buildings . An experimental and experimental and numerical survey, (2015).

[38] S. Ibrahim, M. Ali, B. Baranyai, I. Kistelegdi, Simulation-based analysis of earthen heritage architecture as responsive refugee shelters (Case study: Domes of northern Syria), Int. Arch. Photogramm. Remote Sens. Spat. Inf. Sci. - ISPRS Arch. 54 (2020) 365–372. doi:10.5194/isprs-archives-XLIV-M-1-2020-365-2020.

[39] L. Rincón, A. Carrobé, I. Martorell, M. Medrano, Improving thermal comfort of earthen dwellings in sub-Saharan Africa with passive design, J. Build. Eng. 24 (2019) 100732. doi:10.1016/j.jobe.2019.100732.

[40] S. Thravalou, M. Philokyprou, A. Michael, The impact of window control on thermal performance. investigating adaptable interventions in vernacular mediterranean heritage, J. Archit. Conserv. 24 (2018) 41–59. doi:10.1080/13556207.2018.1456058.

[41] J. Shaeri, M. Yaghoubi, A. Aflaki, A. Habibi, Evaluation of Thermal Comfort in Traditional Houses in a Tropical Climate, Buildings. 8 (2018) 126. doi:10.3390/buildings8090126.

[42] I. Rajapaksha, F. Fiorito, E. Lazer, F. Sartogo, Exploring thermal comfort in the context of historical conservation. A study of the vernacular architecture of Pompeii, Archit. Sci. Rev. 61 (2018) 4–14. doi:10.1080/00038628.2017.1405790.

[43] M. Etxebarria Mallea, L. Etxepare Igiñiz, M. de Luxán García de Diego, Passive hygrothermal behaviour and indoor comfort concerning the construction evolution of the traditional Basque architectural model. Lea valley case study, Build. Environ. 143 (2018) 496–512. doi:10.1016/j.buildenv.2018.06.041.

[44] J. Gupta, M. Chakraborty, A. Paul, V. Korrapatti, A comparative study of thermal performances of three mud dwelling units with courtyards in composite climate, J. Archit. Urban. 41 (2017) 184–198. doi:10.3846/20297955.2017.1355276.

[45] S. Liu, C. Huang, Y. Liu, J. Shen, Z. Li, Retrofitting Traditional Western Hunan Dwellings with Passive Strategies Based on Indoor Thermal Environment, J. Archit. Eng. 24 (2018) 04018017. doi:10.1061/(asce)ae.1943-5568.0000316.

[46] W. Yang, J. Xu, Z. Lu, J. Yan, F. Li, A systematic review of indoor thermal environment of the vernacular dwelling climate responsiveness, 53 (2022).

[47] H.E. Huerto-Cardenas, F. Leonforte, N. Aste, C. Del Pero, G. Evola, V. Costanzo, E. Lucchi, Validation of dynamic hygrothermal simulation models for historical buildings: State of the art, research challenges and recommendations, Build. Environ. 180 (2020) 107081. doi:10.1016/j.buildenv.2020.107081.

[48] ASHRAE Guideline 14-2014, Measurement of Energy, Demand, and Water Savings, ASHRAE Guidel. 14-2014. 4 (2014) 1–150. www.ashrae.org%0Awww.ashrae.org/technology.

[49] FEMP, M&V Guidelines : Measurement and Verification for Federal Energy Projects - Version 3.0, Washington, DC, USA, 2008.

[50] Organization Efficiency Valuation, International Performance Measurement and Verification Protocol: Concepts and Options for Determining Energy and Water Savings, vol. 1, Washington, 2012.

[51] S. Pfenninger, J. DeCarolis, L. Hirth, S. Quoilin, I. Staffell, The importance of open data and software: Is energy research lagging behind?, Energy Policy. 101 (2017) 211–215. doi:10.1016/j.enpol.2016.11.046.

[52] G.R. Ruiz, C.F. Bandera, Validation of calibrated energy models: Common errors, Energies. 10 (2017). doi:10.3390/en10101587.

[53] D. Chakraborty, H. Elzarka, Performance testing of energy models: are we using the right statistical metrics?, J. Build. Perform. Simul. 11 (2018) 433–448. doi:10.1080/19401493.2017.1387607.

[54] I. Costa-Carrapiço, J. Neila González, R. Raslan, Indoor environmental conditions in Vernacular Dwellings in Alentejo, Portugal, Available SSRN Https//Ssrn.Com/Abstract=3965450. (2021). doi:10.2139/ssrn.3944793.

[55] I. Costa-Carrapiço, J. Neila González, R. Raslan, C. Sánchez-Guevara, Understanding thermal comfort in vernacular dwellings in Alentejo, Portugal: a mixed-methods adaptive comfort approach, Available SSRN Https//Ssrn.Com/Abstract=3971717. (2021).

[56] AEMET, IM, Iberian Climate Atlas (1971-2000), 2011.

[57] I. Costa Carrapiço, J.N. González, R. Raslan, C. Sánchez-Guevara, M.D. Redondas Marrero, Understanding thermal comfort in vernacular dwellings in Alentejo, Portugal: A mixed-methods adaptive comfort approach, Build. Environ. 217 (2022) 109084. doi:10.1016/j.buildenv.2022.109084.

[58] BS ISO 9869-1, Thermal insulation - Building elements - In-situ measurement of thermal resistance and thermal transmittance - part 1: Heat flow meter method, BSI Standards Limited 2014, Geneva, Switzerland, 2014.

[59] ISO 6946:2017, Building components and building elements - thermal resistance and thermal transmittance - calculation method., (2017).

[60] E. Lucchi, Thermal transmittance of historical brick masonries: A comparison among standard data, analytical calculation procedures, and in situ heat flow meter measurements, Energy Build. 134 (2017) 171–184. doi:10.1016/j.enbuild.2016.10.045.

[61] M.D. Morris, Factorial sampling plans for preliminary computational experiments, Technometrics. 33 (1991) 161–174. doi:10.1080/00401706.1991.10484804.

[62] P. Heiselberg, H. Brohus, A. Hesselholt, H. Rasmussen, E. Seinre, S. Thomas, Application of sensitivity analysis in design of sustainable buildings, Renew. Energy. 34 (2009) 2030–2036. doi:10.1016/j.renene.2009.02.016.

[63] W. Tian, A review of sensitivity analysis methods in building energy analysis, Renew. Sustain. Energy Rev. 20 (2013) 411–419. doi:10.1016/j.rser.2012.12.014.

[64] S. De Wit, G. Augenbroe, Analysis of uncertainty in building design evaluations and its implications, Energy Build. 34 (2002) 951–958. doi:10.1016/S0378-7788(02)00070-1.

[65] P. Heiselberg, H. Brohus, A. Hesselholt, H. Rasmussen, E. Seinre, S. Thomas, Application of sensitivity analysis in design of sustainable buildings, Renew. Energy. 34 (2009) 2030–2036. doi:10.1016/j.renene.2009.02.016.

[66] V. Corrado, H.E. Mechri, Uncertainty and sensitivity analysis for building energy rating, J. Build. Phys. 33 (2009) 125–156. doi:10.1177/1744259109104884.

[67] Y. Heo, R. Choudhary, G.A. Augenbroe, Calibration of building energy models for retrofit analysis under uncertainty, Energy Build. 47 (2012) 550–560. doi:10.1016/j.enbuild.2011.12.029.

[68] D. Garcia Sanchez, B. Lacarrière, M. Musy, B. Bourges, Application of sensitivity analysis in building energy simulations: Combining first- and second-order elementary effects methods, Energy Build. 68 (2014) 741–750. doi:10.1016/j.enbuild.2012.08.048.

[69] S. Yang, W. Tian, E. Cubi, Q. Meng, Y. Liu, L. Wei, Comparison of Sensitivity Analysis Methods in Building Energy Assessment, Procedia Eng. 146 (2016) 174–181. doi:10.1016/j.proeng.2016.06.369.

[70] G.M. Mauro, M. Hamdy, G.P. Vanoli, N. Bianco, J.L.M. Hensen, A new methodology for investigating the cost-optimality of energy retrofitting a building category, Energy Build. 107 (2015) 456–478. doi:10.1016/j.enbuild.2015.08.044.

[71] A.-T. Nguyen, S. Reiter, P. Rigo, A review on simulation-based optimization methods applied to building performance analysis, Appl. Energy. 113 (2014) 1043–1058. doi:10.1016/j.apenergy.2013.08.061.

[72] T. Wei, A review of sensitivity analysis methods in building energy analysis, Renew. Sustain. Energy Rev. 20 (2013) 411–419. doi:10.1016/j.rser.2012.12.014.

[73] C.A. Pina dos Santos, R. Rodrigues, Coeficientes de transmissão térmica de elementos opacos da envolvente dos edifícios - soluções construtivas de edifícios antiguas. ITE 54., 8th ed., Lisboa, 2017.

[74] I.O. for Standardization, ISO 10456: 2007: Building materials and products: Hygrothermal properties. Tabulated design values and procedures for determining declared and design thermal values, 1 (2017).

[75] B.R. ESTABLISHMENT, Assessing the effects of thermal bridging at junctions and around openings - Information Paper IP 1/06, 2006.

[76] Lawrence Berkeley National Laboratory, DOE2.1E-053 source code, 1994.

[77] T.C. of the P. Environment, ed., ISO 7726, Ergonomics of the thermal environment - Instruments for measuring physical quantities, 2nd ed., 1998.

[78] ASHRAE addedum p to ANSI/ASHRAE Standard 62.1-2013, Ventilation for Acceptable Indoor Air Quality, 2015.

[79] CEN-European Committee for Standardization, EN 17037 European Daylight Standard, 2019. https://velcdn.azureedge.net/~/media/marketing/ee/professional/28mai2019 seminar/veluxen17037tallinn28052019.pdf.

[80] ANSI/ASHRAE 55-2020, Thermal Environmental Conditions for Human Occupancy, Ashrae. (2020) 58. doi:ISSN 1041-2336.

[81] A. Franczyk, Using the Morris sensitivity analysis method to assess the importance of input variables on time-reversal imaging of seismic sources, Acta Geophys. 67 (2019) 1525–1533. doi:10.1007/s11600-019-00356-5.

[82] A. Saltelli, S. Tarantola, F. Campolongo, M. Ratto, Sensitivity analysis in practice: a guide to assessing scientific models, 2004. http://books.google.com/books?id=NsAVmohPNpQC&pgis=1.

[83] I. Costa-Carrapiço, R. Raslan, J.N. González, A systematic review of genetic algorithm-based multi-objective optimisation for building retrofitting strategies towards energy efficiency, Energy Build. 210 (2020). doi:10.1016/j.enbuild.2019.109690.

[84] A.T. Nguyen, S. Reiter, P. Rigo, A review on simulation-based optimization methods applied to building performance analysis, Appl. Energy. 113 (2014) 1043–1058. doi:10.1016/j.apenergy.2013.08.061.

[85] R. Roy, S. Hinduja, R. Teti, Recent advances in engineering design optimisation: Challenges and future trends, CIRP Ann. - Manuf. Technol. 57 (2008) 697–715. doi:10.1016/j.cirp.2008.09.007.

[86] A. Horsley, C. France, B. Quatermass, Delivering energy efficient buildings: a design procedure to demonstrate environmental and economic benefits, Constr. Manag. Econ. 21 (2003) 345–356. doi:10.1080/0144619032000073505.

[87] S.N. Murray, B.P. Walsh, D. Kelliher, D.T.J. O'Sullivan, Multi-variable optimization of thermal energy efficiency retrofitting of buildings using static modelling and genetic algorithms - A case study, Build. Environ. 75 (2014) 98–107. doi:10.1016/j.buildenv.2014.01.011.

[88] E. Asadi, M. Gameiro da Silva, C. Hengeller Antunes, L. Dias, State of the Art on Retrofit Strategies Selection

Using Multi-objective Optimization and Genetic Algorithms, in: F. Torgal, M. Mistretta, A. Kaklauskas, C.. Granqvist (Eds.), Nearly Zero Energy Build. Refurb. A Multidiscip. Approach, Springer, London, UK, 2013: pp. 279–297. doi:10.1007/978-1-4471-5523-2.

[89] C. Diakaki, E. Grigoroudis, D. Kolokotsa, Towards a multi-objective optimization approach for improving energy efficiency in buildings, Energy Build. 40 (2008) 1747–1754. doi:10.1016/j.enbuild.2008.03.002.

[90] J.N. Holst, Using Whole Building Simulation Models and Optimizing Procedures To Optimize Building Envelope Design With Respect To Energy Consumption and Indoor Environment, 8th IBPSA Conf. Eindhoven, Netherlands. (2003) 507–514.

[91] I. García Kerdan, R. Raslan, P. Ruyssevelt, An exergy-based multi-objective optimisation model for energy retrofit strategies in non-domestic buildings, Energy. 117 (2016) 506–522. doi:10.1016/j.energy.2016.06.041.

[92] M. Palonen, M. Hamdy, A. Hasan, MOBO A New Software for Multi-Objective Building Performance Optimization, in: 13th Conf. Int. Build. Perform. Simul. Assoc., Chambéry, France, 2013: pp. 2567–2574.

[93] A. Hasan, M. Vuolle, K. Sirén, Minimisation of life cycle cost of a detached house using combined simulation and optimisation, Build. Environ. 43 (2008) 2022–2034. doi:10.1016/j.buildenv.2007.12.003.

[94] A.M. Rysanek, R. Choudhary, Optimum building energy retrofits under technical and economic uncertainty, Energy Build. 57 (2013) 324–337. doi:10.1016/j.enbuild.2012.10.027.

[95] S. Bandyopadhyay, S. K. Pal, Classification and Learning Using Genetic Algorithms Applications in Bioinformatics, Springer Berlin Heidelberg New York, New York, NY, USA, 2007.

[96] S. Attia, M. Hamdy, W. O'Brien, S. Carlucci, Assessing gaps and needs for integrating building performance optimization tools in net zero energy buildings design, Energy Build. 60 (2013) 110–124. doi:10.1016/j.enbuild.2013.01.016.

[97] Y. Wei, X. Zhang, Y. Shi, L. Xia, S. Pan, J. Wu, M. Han, X. Zhao, A review of data-driven approaches for prediction and classification of building energy consumption, Renew. Sustain. Energy Rev. 82 (2018) 1027–1047. doi:10.1016/j.rser.2017.09.108.

[98] Y. He, N. Liao, J. Bi, L. Guo, Investment decision-making optimization of energy efficiency retrofit measures in multiple buildings under financing budgetary restraint, J. Clean. Prod. 215 (2019) 1078–1094. doi:10.1016/j.jclepro.2019.01.119.

[99] D.F. Jones, S.K. Mirrazavi, M. Tamiz, Multi-objective meta-heuristics: An overview of the current state-of-the-art, Eur. J. Oper. Res. 137 (2002) 1–9. doi:10.1016/S0377-2217(01)00123-0.

[100] L. Chambers, The Practical Handbook of GENETIC ALGORITHMS: Applications, Chapman & Hall/CRC, New York, NY, USA, 2001.

[101] W. Wang, R. Zmeureanu, H. Rivard, Applying multi-objective genetic algorithms in green building design optimization, Build. Environ. 40 (2005) 1512–1525. doi:10.1016/j.buildenv.2004.11.017.

[102] R. Charron, A. Athienitis, The use of genetic algorithms for a net-zero energy solar home design optimisation tool, (2006) I215–I220. http://www.scopus.com/inward/record.url?eid=2-s2.0-84865713840&partnerID=40&md5=856eb02fd2f6aa91cc84578bc856b4df.

[103] M. Hamdy, A. Hasan, K. Siren, Applying a multi-objective optimization approach for Design of low-emission cost-effective dwellings, Build. Environ. 46 (2011) 109–123. doi:10.1016/j.buildenv.2010.07.006.

[104] G. Said, A. Mahmoud, E.-S. El-Horbaty, A Comparative Study of Meta-heuristic Algorithms for Solving Quadratic Assignment Problem, Int. J. Adv. Comput. Sci. Appl. 5 (2014) 1–6. doi:10.14569/ijacsa.2014.050101.

[105] F. Ascione, N. Bianco, C. De Stasio, G.M. Mauro, G.P. Vanoli, Multi-stage and multi-objective optimization for energy retrofitting a developed hospital reference building: A new approach to assess cost-optimality, Appl. Energy. 174 (2016) 37–68. doi:10.1016/j.apenergy.2016.04.078.

[106] Y. Fan, X. Xia, Energy-efficiency building retrofit planning for green building compliance, Build. Environ. 136 (2018) 312–321. doi:10.1016/j.buildenv.2018.03.044.

[107] R. Evins, A review of computational optimisation methods applied to sustainable building design, Renew. Sustain. Energy Rev. 22 (2013) 230–245. doi:10.1016/j.rser.2013.02.004.

[108] R.A. Lara, E. Naboni, G. Pernigotto, F. Cappelletti, Y. Zhang, F. Barzon, A. Gasparella, P. Romagnoni, Optimization Tools for Building Energy Model Calibration, Energy Procedia. 111 (2017) 1060–1069.

doi:10.1016/j.egypro.2017.03.269.

[109] F. Ascione, N. Bianco, G. Mauro, D. Napolitano, G. Vanoli, A Multi-Criteria Approach to Achieve Constrained Cost-Optimal Energy Retrofits of Buildings by Mitigating Climate Change and Urban Overheating, Climate. 6 (2018) 37. doi:10.3390/cli6020037.

[110] H. Son, C. Kim, Evolutionary many-objective optimization for retrofit planning in public buildings: A comparative study, J. Clean. Prod. 190 (2018) 403–410. doi:10.1016/j.jclepro.2018.04.102.

[111] F. Ascione, N. Bianco, G.M. Mauro, D.F. Napolitano, Retrofit of villas on Mediterranean coastlines: Pareto optimization with a view to energy-efficiency and cost-effectiveness, Appl. Energy. 254 (2019) 113705. doi:10.1016/j.apenergy.2019.113705.

[112] X. Shi, Z. Tian, W. Chen, B. Si, X. Jin, A review on building energy efficient design optimization rom the perspective of architects, Renew. Sustain. Energy Rev. 65 (2016) 872–884. doi:10.1016/j.rser.2016.07.050.

[113] V. Machairas, A. Tsangrassoulis, K. Axarli, Algorithms for optimization of building design: A review, Renew. Sustain. Energy Rev. 31 (2014) 101–112. doi:10.1016/j.rser.2013.11.036.

[114] A. Konak, D.W. Coit, A.E. Smith, Multi-objective optimization using genetic algorithms: A tutorial, Reliab. Eng. Syst. Saf. 91 (2006) 992–1007. doi:10.1016/j.ress.2005.11.018.

[115] S. Longo, F. Montana, E. Riva Sanseverino, A review on optimization and cost-optimal methodologies in low-energy buildings design and environmental considerations, Sustain. Cities Soc. 45 (2019) 87–104. doi:10.1016/j.scs.2018.11.027.

[116] I. García Kerdan, R. Raslan, P. Ruyssevelt, D. Morillón Gálvez, A comparison of an energy/economic-based against an exergoeconomic-based multi-objective optimisation for low carbon building energy design, Energy. 128 (2017) 244–263. doi:10.1016/j.energy.2017.03.142.

[117] P. Shen, W. Braham, Y. Yi, E. Eaton, Rapid multi-objective optimization with multi-year future weather condition and decision-making support for building retrofit, Energy. 172 (2019) 892–912. doi:10.1016/j.energy.2019.01.164.

[118] C. Coello, An updated survey of GA-based multiobjective optimization techniques, ACM Comput. Surv. 32 (2000) 109–143. doi:10.1145/358923.358929.

[119] K. Deb, Multi-objective Optimization using Evolutionary Algorithms, John Wiley & Sons, New York, NY, USA, 2001.

[120] D. Goldberg, Genetic algorithms in search, optimization, and machine learning, Reading (Massachusetts), 1989.

[121] I. García Kerdan, R. Raslan, P. Ruyssevelt, Parametric study and simulation-based exergy optimization for energy retrofits in buildings, 28TH Int. Conf. Effic. Cost, Optim. Simul. Environ. Impact Energy Syst. (2015).

[122] J.H. Holland, Adaptation in natural and artificial systems, 1992. doi:10.1086/418447.

[123] J. Bouillot, Climatic design of vernacular housing in different provinces of China, J. Environ. Manage. 87 (2008) 287–299. doi:10.1016/j.jenvman.2006.10.029.

[124] H. Spencer, The Principles of Biology, London, Edinburgh, Dublin Philos. Mag. J. Sci. I (1864) 444. doi:10.5962/bhl.title.1472.

[125] F. Ascione, N. Bianco, R.F. De Masi, G.M. Mauro, G.P. Vanoli, Resilience of robust cost-optimal energy retrofit of buildings to global warming: A multi-stage, multi-objective approach, Energy Build. 153 (2017) 150–167. doi:10.1016/j.enbuild.2017.08.004.

[126] F. Ascione, N. Bianco, C. De Stasio, G.M. Mauro, G.P. Vanoli, A new methodology for cost-optimal analysis by means of the multi-objective optimization of building energy performance, Energy Build. 88 (2015) 78–90. doi:10.1016/j.enbuild.2014.11.058.

[127] G.M. Mauro, C. Menna, U. Vitiello, D. Asprone, F. Ascione, N. Bianco, A. Prota, G.P. Vanoli, A multi-step approach to assess the lifecycle economic impact of seismic risk on optimal energy retrofit, Sustainability. 9 (2017). doi:10.3390/su9060989.

[128] S.F. Tadeu, R.F. Alexandre, A.J.B. Tadeu, C.H. Antunes, N.A. V Simões, P.P. Da Silva, A comparison between cost optimality and return on investment for energy retrofit in buildings-A real options perspective, Sustain. Cities Soc. 21 (2016) 12–25. doi:10.1016/j.scs.2015.11.002.

[129] F. Ascione, N. Bianco, R.F. De Masi, G.M. Mauro, G.P. Vanoli, Energy retrofit of educational buildings: Transient energy simulations, model calibration and multi-objective optimization towards nearly zero-energy performance, Energy Build. 144 (2017) 303–319. doi:10.1016/j.enbuild.2017.03.056.

[130] F. Ascione, N. Bianco, Villas on Islands: cost-effective energy refurbishment in Mediterranean coastline houses, Energy Procedia. 159 (2019) 192–200. doi:10.1016/j.egypro.2018.12.050.

[131] L.G. Caldas, L.K. Norford, A design optimization tool based on a genetic algorithm, Autom. Constr. 11 (2002) 173–184.

[132] E.M. Malatji, J. Zhang, X. Xia, A multiple objective optimisation model for building energy efficiency investment decision, Energy Build. 61 (2013) 81–87. doi:10.1016/j.enbuild.2013.01.042.

[133] G. Ramos Ruiz, C. Fernández Bandera, T. Gómez-Acebo Temes, A. Sánchez-Ostiz Gutierrez, Genetic algorithm for building envelope calibration, Appl. Energy. 168 (2016) 691–705. doi:10.1016/j.apenergy.2016.01.075.

[134] E. Asadi, M.G. Da Silva, C.H. Antunes, L. Dias, Multi-objective optimization for building retrofit strategies: A model and an application, Energy Build. 44 (2012) 81–87. doi:10.1016/j.enbuild.2011.10.016.

[135] I. García Kerdan, R. Raslan, P. Ruyssevelt, D. Morillón Gálvez, ExRET-Opt: An automated exergy/exergoeconomic simulation framework for building energy retrofit analysis and design optimisation, Appl. Energy. 192 (2017) 33–58. doi:10.1016/j.apenergy.2017.02.006.

[136] R. Batres, Generating operating procedures using a micro genetic algorithm, 31 (n.d.). doi:10.1016/B978-0-444-59506-5.50094-8.

[137] H. Breesch, A. Janssens, Building simulation to predict the performances of natural night ventilation: Uncertainty and sensitivity analysis, IBPSA 2005 - Int. Build. Perform. Simul. Assoc. 2005. (2005) 115–122.

[138] I.O. for Standardization, ISO 6781:1983 - Thermal Insulation - Qualitative detection of thermal irregularities in building envelopes - Infrared method, 1983.